TWEAK–Fn14–RelB Signaling Cascade Promotes Stem Cell–like Features that Contribute to Post-Chemotherapy Ovarian Cancer Relapse

Ryne Holmberg[1], Mikella Robinson[2], Samuel F. Gilbert[2], Omar Lujano-Olazaba[2], Jennifer A. Waters[2], Emily Kogan[2], Candyd Lace R. Velasquez[2], Denay Stevenson[1], Luisjesus S. Cruz[2], Logan J. Alexander[2], Jacqueline Lara[2], Emily M. Mu[2], Jared Rafael Camillo[2], Benjamin G. Bitler[3], Tom Huxford[1], and Carrie D. House[2,4]

ABSTRACT

Disease recurrence in high-grade serous ovarian cancer may be due to cancer stem–like cells (CSC) that are resistant to chemotherapy and capable of reestablishing heterogeneous tumors. The alternative NF-κB signaling pathway is implicated in this process; however, the mechanism is unknown. Here we show that TNF-like weak inducer of apoptosis (TWEAK) and its receptor, Fn14, are strong inducers of alternative NF-κB signaling and are enriched in ovarian tumors following chemotherapy treatment. We further show that TWEAK enhances spheroid formation ability, asymmetric division capacity, and expression of *SOX2* and epithelial-to-mesenchymal transition genes *VIM* and *ZEB1* in ovarian cancer cells, phenotypes that are enhanced when TWEAK is combined with carboplatin. Moreover, TWEAK in combination with chemotherapy induces expression of the CSC marker CD117 in CD117$^-$ cells. Blocking the TWEAK–Fn14–RelB signaling cascade with a small-molecule inhibitor of Fn14 prolongs survival following carboplatin chemotherapy in a mouse model of ovarian cancer. These data provide new insights into ovarian cancer CSC biology and highlight a signaling axis that should be explored for therapeutic development.

Implications: This study identifies a unique mechanism for the induction of ovarian cancer stem cells that may serve as a novel therapeutic target for preventing relapse.

Introduction

Ovarian cancer is the most deadly gynecologic malignancy in the United States, resulting in over 15,000 deaths each year (1). Although most high-grade serous ovarian cancer (HGSOC) patients initially respond to platinum-based chemotherapy, over 80% of patients with advanced-stage disease relapse within 24 months and eventually develop chemoresistance (2). Thus, much research has focused on clarifying mechanisms of chemoresistance and the processes involved in tumor relapse. Over a decade of research has implicated tumor-initiating cells, here referred to as cancer stem–like cells (CSC), in mediating these activities; efforts to characterize and target these cells are a promising avenue for preventing relapse and improving survival for women with ovarian cancer (3–9).

As a master regulator of several cellular processes including proliferation, apoptosis, and immune response, the NF-κB signaling network has a central role in cancer progression (10, 11) and contributes to metastasis and poor outcomes in ovarian cancer (12–15). NF-κB follows classic (canonical) or alternative (noncanonical) signaling pathways leading to activation of either p65(RelA):p50 or RelB:p52 NF-κB heterodimers, respectively. Whereas induction of NF-κB activity through the classic pathway is rapid, transient, and typically a consequence of inflammatory cytokines such as TNFα, IL1β, IL6, and IL8, alternative pathway signaling promotes more delayed and persistent NF-κB activity in response to cytokines such as LT-β, TWEAK, CD40, BAFF, and RANK (16, 17). Although classic NF-κB signaling has been observed previously in ovarian cancers, involvement of NF-κB through the alternative pathway has been investigated only recently (17–20). For example, one recent study examining 196 ovarian cancer tissues found that p52 expression, independent of p65, is associated with significantly lower progression-free and overall survival (19).

Our previous work implicates alternative NF-κB in maintaining ovarian cancer CSC phenotypes (18). Relative to 2-D monolayer-cultured cells, 3-D cultured cells exhibit stem-like properties including enhanced tumor initiation and chemoresistance, elevated expression of *SOX2*, *OCT4*, and *NANOG* genes, and an enrichment of CD117, CD44, and CD133 surface markers and aldehyde-dehydrogenase (ALDH) activity (9, 18, 21). We found that these cells exhibit increased activation of both classic and alternative NF-κB pathways that promote either a proliferative or quiescent phenotype, respectively (18).

Given its ubiquitous activity and pleiotropic effects on a variety of normal cells, targeting NF-κB has remained clinically unfeasible. However, identifying and targeting specific inducers of this pathway

[1]Department of Chemistry, San Diego State University, San Diego, California. [2]Department of Biology, San Diego State University, San Diego, California. [3]Department of Obstetrics and Gynecology, University of Colorado, Aurora, Colorado. [4]Moores Cancer Center, University of California San Diego, La Jolla, California.

R. Holmberg and M. Robinson contributed equally to this work as co-first authors.

Corresponding Author: Carrie D. House, Biology, San Diego State University, 5500 Campanile Drive, Shiley Bioscience Center 2104, San Diego, CA 92182. Phone: 619-594-3053; E-mail: cdhouse@sdsu.edu

Mol Cancer Res 2023;21:170–86

doi: 10.1158/1541-7786.MCR-22-0486

is a promising approach. The upstream activators of alternative NF-κB signaling in ovarian cancer are unclear but include a variety of factors from the inflammatory but immunosuppressive tumor microenvironment (TME) that characterizes this disease (14). To begin to elucidate these, we investigated the hypothesis that specific inducers of alternative NF-κB are enriched in the ovarian TME and contribute to disease progression and relapse through induction of NF-κB activity. We show that TNF-like weak inducer of apoptosis (TWEAK), a multifunctional cytokine important for tissue repair, is enriched following chemotherapy, induces activation of alternative NF-κB, enhances stem-like features, and contributes to relapse in an ovarian cancer mouse model. This study provides novel insight into NF-κB signaling and CSC biology and uncovers a potential new therapeutic target for inhibiting relapse in ovarian cancer.

Materials and Methods

General cell culture conditions

Cell line information is presented in Supplementary Table S1. OVCAR8 and CAOV4 cells were obtained and authenticated from NCI-Frederick DCTD tumor/cell line repository. OV90 was obtained and authenticated by ATCC. Deidentified ascites specimen VBCF004 was collected as pathologic waste from posttreatment ovarian cancer patients and was determined to be outside the federal regulations for the protection of human subjects (45 CFR 46; OHSRP #12727 and #12797; ref. 18). Viable tumor cells and non-cell fractions from ascites were purified using Ficoll separation as previously reported (18). All adherent cultures were maintained in standard media (RPMI for OVCAR8, OV90, and CAOV4; DMEM:F12 for VBCF004), supplemented with 10% FBS and 1% 10,000 U/mL penicillin/streptomycin. When using inducible CRISPR-Cas9 cell lines, tetracycline-free FBS was substituted for standard FBS. Cells are tested for *mycoplasma* annually. Cells were maintained in culture for a maximum of 15 passages.

Molecules

TWEAK (human and mouse), BAFF, CD40L, CRP, IL1β, IL6, IL8, Leptin, TGFβ1, TGFβ3, and TNFα cytokines were purchased from R&D Systems and reconstituted per the manufacturer's instructions (Supplementary Table S1). Carboplatin for *in vitro* assays was reconstituted per the manufacturer's instructions (R&D Systems; Supplementary Table S1). The FN14 inhibitor L542-0366 was reconstituted in DMSO with sonication until dissolved per experiment (Millipore; Supplementary Table S2).

NF-κB luciferase assay

The NF-κB Luciferase Cignal Lenti Reporter Assay was purchased from Qiagen, transduced per the manufacturer's protocol at MOI of 50, selected with 2 μg/mL puromycin, and expanded to generate stably expressing reporter cell lines. Cells were plated in 96-well, opaque white, clear-bottom plates at 1,500–6,000 cells/well depending on cell line with cytokines added the following day. The cells were allowed to incubate for 24 hours before analysis using the Promega ONE-Glo EX Luciferase Assay System per the manufacturer's protocol. Luminescence was read on a SpectraMax iD3 plate reader.

NF-κB binding assay

Cells were plated in 10-cm dishes and allowed to rest overnight before the addition of TWEAK for either 2 or 24 hours. NF-κB proteins were quantified in whole-cell lysates using the TransAM NF-κB Activation Assay from Active Motif per the manufacturer's instructions.

Western blots

Cells were plated in culture dishes and allowed to rest overnight before treatment. Whole-cell lysates were collected using NP-40 cell lysis buffer with HALT protease and phosphatase inhibitor. Nuclear and cytosolic fractions were collected using Active Motif Nuclear Extract Kit per the manufacturer's instructions. Proteins were separated by SDS-PAGE using 4%–12% Bis-Tris gels and MOPS running buffer and transferred to a PVDF membrane before blocking and incubation overnight at 4°C with primary antibodies (Supplementary Table S2). Secondary antibodies were incubated for 1 hour at room temperature (Supplementary Table S2). Bands were visualized on the Invitrogen iBright CL1000 Imaging System with analysis using the iBright Analysis Software.

Cell viability assay

Cells were seeded into 96-well, opaque white, clear-bottom plates and allowed to rest overnight before being treated with TWEAK and allowed to grow for 72 hours. Viability was assessed after 72 hours with CellTiter-Glo 2.0 reagent per the manufacturer's instructions. Luminescence was detected using a SpectraMax iD3 plate reader.

Proliferation

For Ki-67, cells were seeded into culture dishes and incubated overnight before treatment with TWEAK for 72 hours. Cells were then fixed in 1% formalin followed by Triton-X permeabilization. Cells were stained with primary antibody to Ki-67 followed by secondary antibody (Supplementary Table S2) and quantified by flow cytometry.

For EdU, 500 to 1,000 cells were seeded into black 96-well, clear-bottom plates overnight prior to treatment with TWEAK and EdU for 72 hours. EdU incorporation was assessed with the Click-iT Plus EdU Alexa Fluor 647 assay per the manufacturer's instructions. Hoechst 33342 and EdU incorporation were imaged on the ImageXpress Pico plate imager and analyzed with CellReporterXpress software (Supplementary Table S2).

TUNEL assay

2,500 to 4,000 cells were seeded into black 96-well, clear-bottom plates and incubated overnight prior to treatment with either vehicle, TWEAK, or carboplatin and allowed to incubate for 6 hours. EdUTP incorporation was assessed with the Click-iT Plus TUNEL Alexa Fluor 488 assay per the manufacturer's instructions. Hoechst 33342 and EdUTP incorporation were imaged on the Molecular Devices ImageXpress Pico plate imager and analyzed with CellReporterXpress software. Percent EdUTP incorporation was quantified blindly using automated imaging analysis with CellProfiler for counting and scoring (22).

Caspase assay

Cells were plated into black 96-well, clear-bottom plates and incubated overnight prior to treatment with either vehicle, TWEAK, or carboplatin and incubated for 72 hours. Caspase-3/7 activity was assessed using the Invitrogen CellEvent Caspase-3/7 Green Detection Reagent per the manufacturer's instructions (Supplementary Table S2). Hoechst 33342 and caspase-3/7 cleavage was imaged on the Molecular Devices ImageXpress Pico plate imager and analyzed with CellReporterXpress software.

RNA extraction and quantitative reverse transcription PCR (qRT-PCR)

Total RNA was isolated using the NucleoSpin RNA Plus kit per the manufacturer's instructions. cDNA synthesis was carried out using the High-Capacity cDNA Reverse Transcription kit per the manufacturer's protocol. Quantitation and normalization of gene expression were performed using TaqMan Fast Advanced Master Mix and TaqMan probes (Supplementary Table S2). Experiments were run on a QuantStudio 3 instrument and analyzed with the QuantStudio Design and Analysis software using the delta-delta Ct method with *GAPDH* endogenous control.

Spheroid formation assay

Cells were plated at 100 to 500 cells/well in ultra-low attachment, flat bottom 96-well plates cultured in RPMI media supplemented with 5% to 10% FBS, 1% 10,000 U/mL penicillin/streptomycin, and either TWEAK or vehicle. Spheroids were allowed to grow for 4 to 7 days, with TWEAK supplementation every 3 to 4 days, followed by staining with Hoechst 33342. Spheroids were imaged using the ImageXpress Pico and size 50 to 500 μm were counted using the CellReporterXpress software (Supplementary Table S2). Spheroid efficiency is defined as (# of spheroids)/(# of cells per well).

Pulse-chase assay

Cells were plated at 500 to 3,000 cells per well in a 96-well, black well, clear-bottom plate and allowed to rest overnight. For the pulse, cells were grown for at least two divisions in 0.5 to 1 μmol/L EdU prior to the chase, in which cells were removed from EdU and allowed to divide in the presence of either TWEAK or vehicle for 60 to 72 hours. EdU incorporation was assessed with the Click-iT Plus EdU Alexa Fluor 647 assay and F-actin was also assessed using Phalloidin-Alexa Fluor 488, both used per the manufacturer's instructions. Hoechst 33342 and EdU incorporation or F-actin staining were imaged on the Molecular Devices ImageXpress Pico plate imager and analyzed with CellReporterXpress software (Supplementary Table S2).

siRNA transfections

Cells were plated the day before to achieve a confluency of around 60% for transfection. 30 nmol/L pools of 4 siRNAs targeting either *FN14* or a nontargeting control were transfected using Lipofectamine RNAiMAX per the manufacturer's instructions (Supplementary Table S2). Cells were incubated for 24 hours before being collected for downstream experiments. Cells were replated and cultured for an additional 48 hours for validation of Fn14 silencing.

CRISPR cell line production

Knockout clonal cell lines for RelB were derived per the manufacturer's protocol for Horizon's Edit-R Inducible Lentiviral Cas9 Nuclease with Edit-R Lentiviral sgRNA (Supplementary Table S2). 10 μg/mL blasticidin and 2 μg/mL puromycin was used to select for cells with the integrated Cas9 nuclease and sgRNA guides followed by induction of genomic editing with 3 μg/mL doxycycline for 7 days. Serially diluted clonal lines were expanded and screened for the loss of RelB by western blot.

Flow cytometry and CD117 sorting

Flow cytometry experiments were completed as previously described (ref. 9; Supplementary Table S2). For sorting experiments, CAOV4 cells were seeded for 6 days in ultra-low attachment T-75 cm^2 flasks with stem cell media (DMEM/F12, 1% knockout serum replacement, 0.4% BSA, 0.1% insulin-transferrin-selenium-X (ITS), 1% 10,000 U/mL penicillin/streptomycin and supplemented every 2 to 3 days with 20 ng/mL EGF and 10 ng/mL FGF). After 6 days, cells were collected and prepared into single-cell suspensions using CellStripper Dissociation Reagent and needle dissociation using a 25-gauge needle. Cells were stained for CD117 or propidium iodide (PI), sorted for $CD117^-$ and/or $CD117^+$ cells using the BD FACSMelody Cell Sorter, and then plated for 24 hours prior to treatment with either vehicle, TWEAK, carboplatin, or TWEAK and carboplatin (Supplementary Table S2). For assessing gene expression, $CD117^+$ or $CD117^-$ cells were harvested after 72 hours of treatment with TWEAK and immediately processed for downstream qRT-PCR. For assessing viability, $CD117^+$ cells were harvested after 120 hours and processed for the cell viability assay as described above. 120-hour treatments consisted of 72 hours carboplatin followed by 48 hours vehicle; 72 hours carboplatin and TWEAK followed by 48 hours vehicle; 48 hours TWEAK followed by 72 hours carboplatin; or 72 hours carboplatin followed by 48 hours TWEAK. For assessing marker expression of CD117 in sorted cells, either mock sorted or $CD117^-$ cells were cultured for 14 days with two doses of sequential treatments of vehicle or carboplatin and TWEAK, as previously reported (9). Briefly, cells received an initial treatment of carboplatin and TWEAK for 24 hours with subsequent 2-fold dilution with media.

To assess CD117 growth characteristics and chemoresistance, OV90 cells were enriched for $CD117^+$ and $CD117^-$ using the Miltenyi Biotec CD117 microbead kit and the quadroMACS separator with LS columns. Separated cell populations were either plated for cell viability assay or for spheroid formation assay as described above.

Animal experiments

All animal studies were approved by the SDSU Animal Care and Use Committee (protocol approval numbers 18-04-006H and 21-05-003H). Power analysis indicates using 6 to 8 mice/group to achieve a conservative effect size of 0.4. For subcutaneous xenografts, 50,000 to 500,000 OV90 cells in 1:1 Matrigel in PBS were subcutaneously injected into the left flank of 8-week-old female athymic Nu/Nu mice. Mice were weighed, and tumors were measured with blinded groups twice weekly. Once tumors reached 150 mm^3, mice were treated with either vehicle or carboplatin (50 mg/kg) delivered via intraperitoneal (i.p.) injection once per week for 3 weeks. Mice were sacrificed in two groups: on average 5 days (group 1) or 12 days (group 2) after the third dose of carboplatin to evaluate progressive changes.

For i.p. xenografts, 4×10^6 CAOV4 cells in 500 μL PBS were injected into 8-week-old female athymic Nu/Nu mice. Mice were weighed and monitored for clinical signs twice weekly. Tumor formation was assessed by palpation and visual inspection of the abdomen. Seven days after injection, mice were randomly assigned to either group 1: vehicle, group 2: carboplatin (50 mg/kg) i.p. once per week for 3 weeks, group 3: carboplatin (as administered in group 2) combined with FN14 inhibitor (9 mg/kg) in 5% DMSO/95% corn oil delivered by i.p. every other day for 3 weeks, or group 4: carboplatin (as administered in group 2) followed by FN14 inhibitor (as administered in group 3) for 6 weeks or until humane endpoints. Tumor burden for mice was assessed after necropsy with collection of peritoneal wall, spleen, liver, omentum, spleen, mesentery, ovaries, and diaphragm. To avoid endpoint bias, mice were blinded to treatment groups, randomized to separate cages, weighed

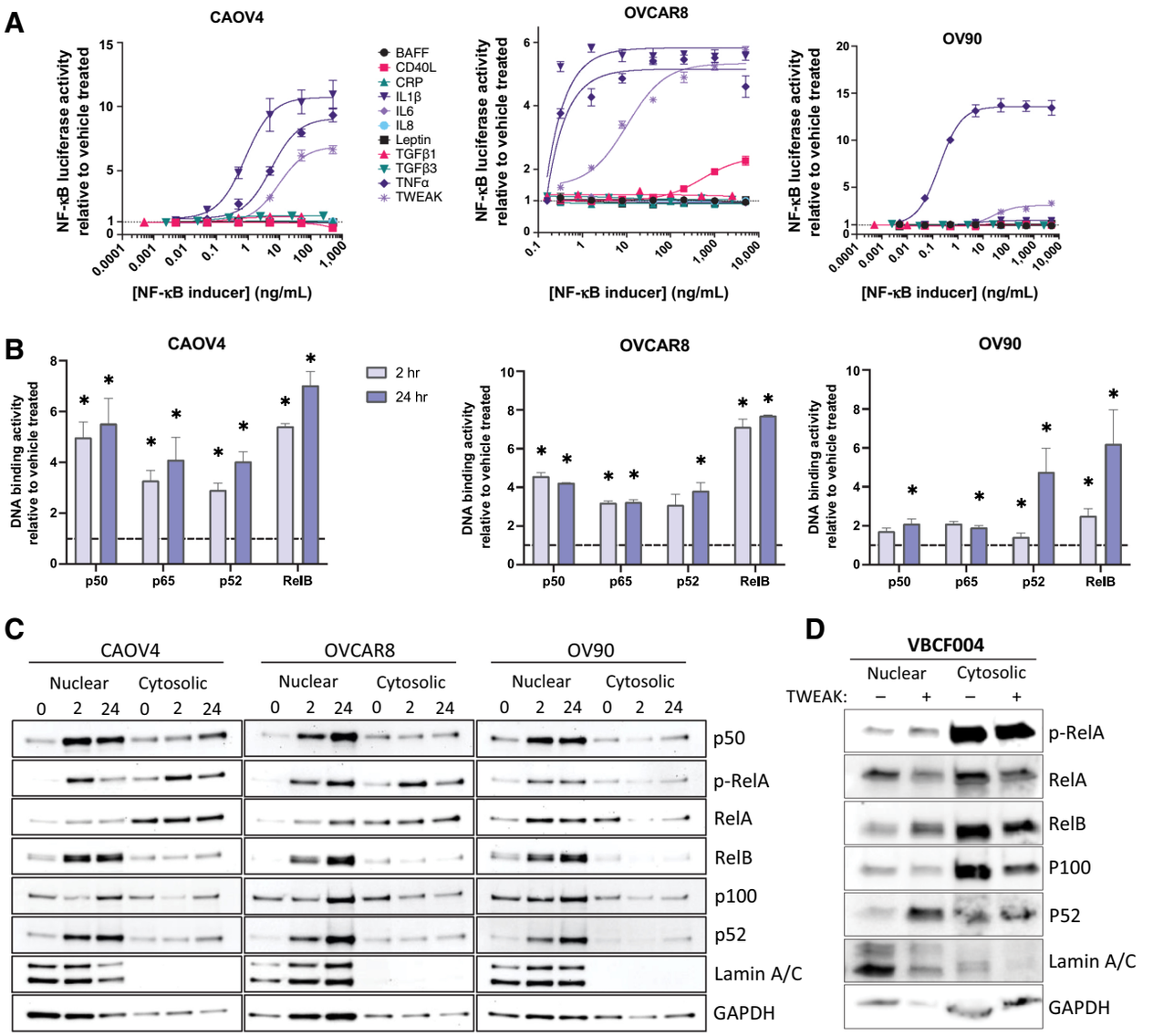

Figure 1.

TWEAK activates classic and alternative NF-κB pathways in ovarian cancer cell lines and patient-derived cells. **A,** Luciferase reporter assay showing NF-κB activity in response to 24-hour stimulation with different cytokines ($n = 3$). **B,** DNA-binding of NF-κB proteins with TWEAK stimulation (25 ng/mL) for 2 or 24 hours relative to vehicle. One-way ANOVA with Dunnett *post hoc* test ($n = 3$). **C,** Nuclear and cytosolic western blots of NF-κB proteins with TWEAK (25 ng/mL, 0, 2, or 24 hours) in CAOV4, OVCAR8, and OV90. **D,** Nuclear and cytosolic western blots of NF-κB proteins with TWEAK (100 ng/mL, 24 hours) stimulation in ascites sample VBCF004. Data represent mean and SEM. *, $P < 0.05$.

twice weekly, and assessed for survival endpoints four times a week by the same observer.

Enzyme-linked immunosorbent assay (ELISA)

The concentration of cytokines IL6 and TWEAK (Supplementary Table S2) was assessed using DuoSet sandwich ELISA per the manufacturer's instruction using non-cell fractions from ascites samples and tumor tissue samples, which were flash frozen immediately following collection. For the tissue, 1 to 3 mg sections were dissected, weighed, and protein was dissociated on gentleMACS M tubes in RIPA lysis buffer. Samples were prepared and analyzed per the manufacturer's instructions.

IHC and immunofluorescence (IF)

For IHC, tumors were resected, fixed in 10% neutral buffered formalin, and stored in 70% ethanol before processing. Tumors were embedded in paraffin and sectioned at 5 μm. Antigen retrieval was performed in citrate buffer and quenched with

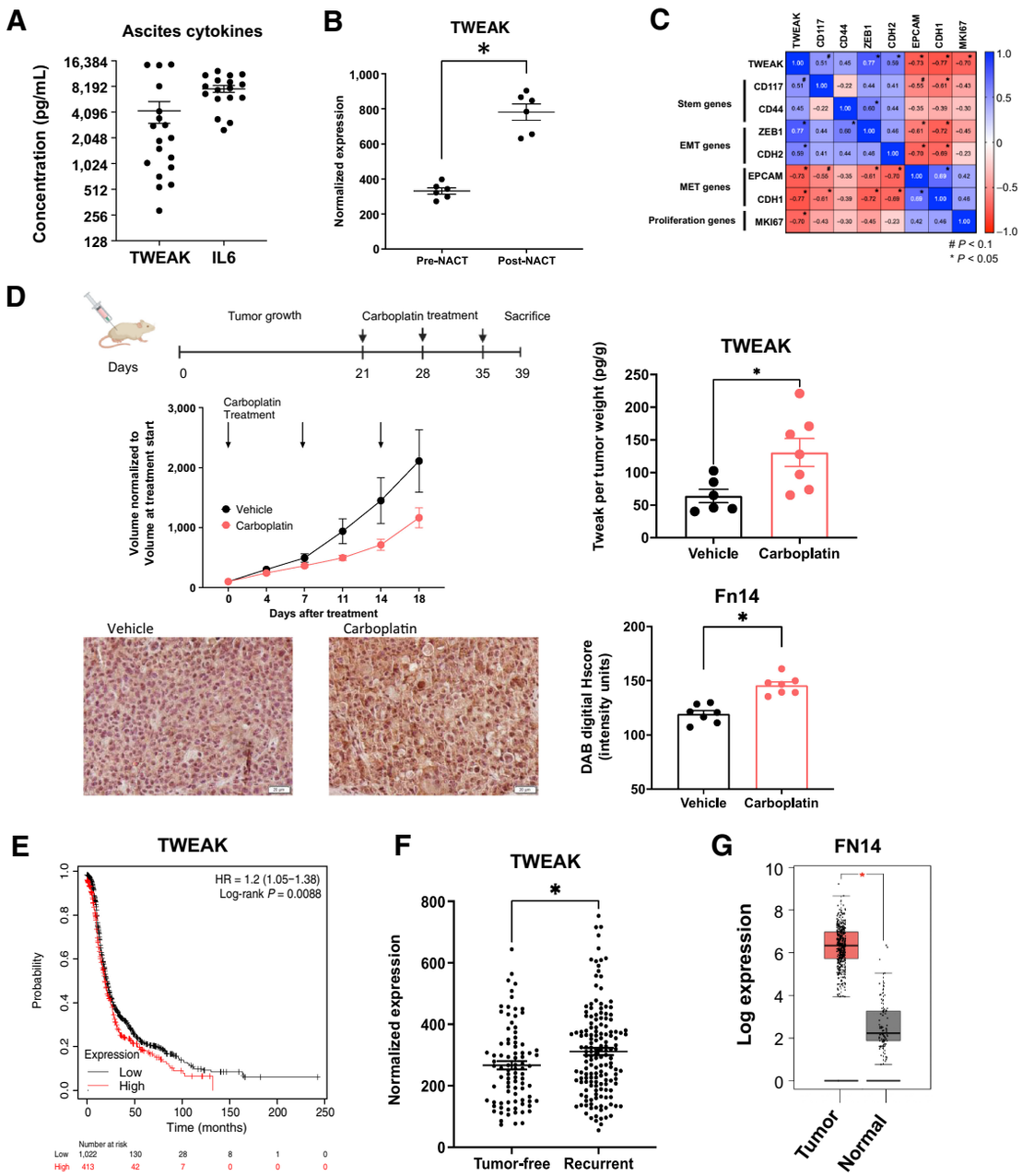

Figure 2.

Following chemotherapy, TWEAK and its receptor, Fn14, are significantly elevated in patient samples and mouse tumors. **A,** TWEAK and IL6 concentration in noncellular ascites fraction collected from recurrent HGSOC patients ($n = 18$). **B,** TWEAK gene expression in ovarian cancer tumors collected pre- and post-neoadjuvant chemotherapy (NACT). Paired *t* test ($n = 6$). **C,** Pearson correlation of select genes to TWEAK expression for all collected samples (pre- and post-NACT; $n = 6$). **D,** Subcutaneous tumors were generated in nude mice using OV90 cells. Tumors were allowed to grow for 21 days followed by 3 cycles of carboplatin (50 mg/kg) or vehicle and resected 5 days after the final carboplatin treatment. Experimental design created with BioRender.com (top). Tumor volume was measured twice weekly and graphed normalized to the volume at treatment start (center, left). TWEAK concentration per tumor weight measured using ELISA (center, right). Unpaired *t* test ($n = 6, 7$). Fixed tumor fractions were histologically stained for Fn14. Representative images (bottom, left) and Fn14 digital H score quantification using ImageJ (bottom, right). Unpaired *t* test ($n = 7, 7$). **E,** Kaplan–Meier plots from KMPlotter comparing high expression (red) and low expression (black) of TWEAK and associated progression-free survival (PFS) of ovarian cancer patients ($n = 1{,}435$). **F,** TCGA analysis of TWEAK in tumors from HGSOC patients who recurred (tumor <5 years after follow-up) or remained tumor-free. Unpaired *t* test ($n = 585$). **G,** FN14 gene expression by Gepia2 of normal ovarian surface epithelium (black) and ovarian tumor (red). Unpaired *t* test ($n = 88$ normal, $n = 426$ tumor). Data represent mean and SEM. *, $P < 0.05$.

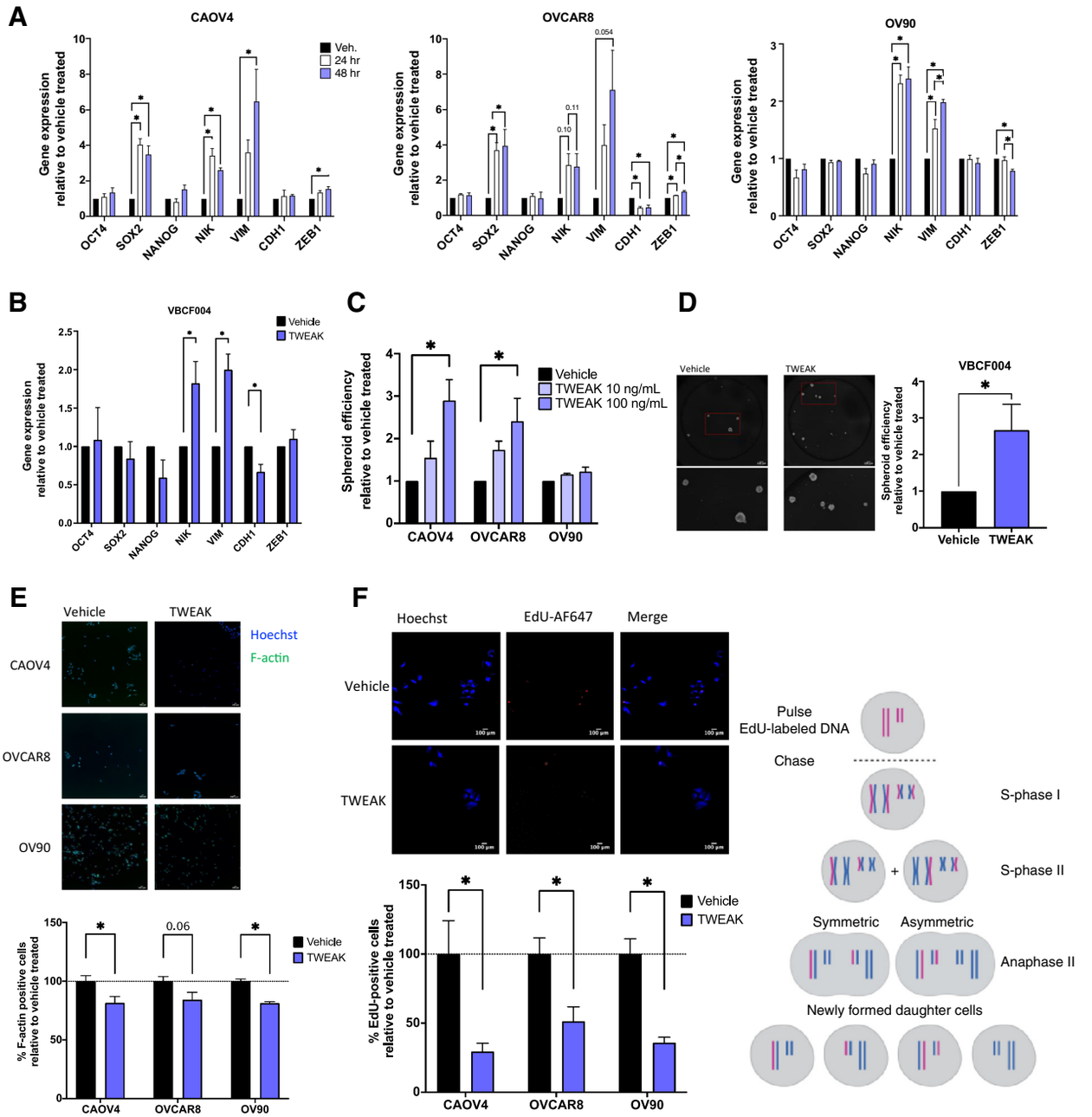

Figure 3.

TWEAK stimulation enhances the development of stem-like features in ovarian cancer cell lines and patient-derived cells. **A,** qRT-PCR for select stemness and EMT genes in HGSOC cells with vehicle or TWEAK treatment (100 ng/mL) for 24 or 48 hours. One-way ANOVA with Tukey *post hoc* test ($n = 3$). **B,** qRT-PCR on ascites-derived cells VBCF004 for select stemness and EMT genes with TWEAK treatment (100 ng/mL) for 48 hours. Unpaired *t* test ($n = 3$). **C,** Spheroid efficiency of HGSOC cell lines with TWEAK treatment (10 or 100 ng/mL) relative to the vehicle for 6 days. One-way ANOVA, Dunnett *post hoc* test ($n = 4$). **D,** Spheroid efficiency of ascites-derived cells VBCF004 with TWEAK treatment (100 ng/mL) relative to vehicle for 4 days. Representative images (left) and quantification with Hoechst (right). Unpaired *t* test ($n = 3$). **E,** F-actin staining of HGSOC cells with TWEAK (100 ng/mL) treatment for 72 hours. Representative images (top) and quantification per well relative to vehicle treated (bottom). Unpaired *t* test ($n = 6$). **F,** EdU incorporation pulse-chase assay of HGSOC cells with TWEAK (100 ng/mL) treatment for 72 hours. Experimental design created with BioRender.com (top), representative images (center), and quantification per well relative to vehicle treated (bottom). Unpaired *t* test ($n = 6$). Data represent mean and SEM. *, $P < 0.05$.

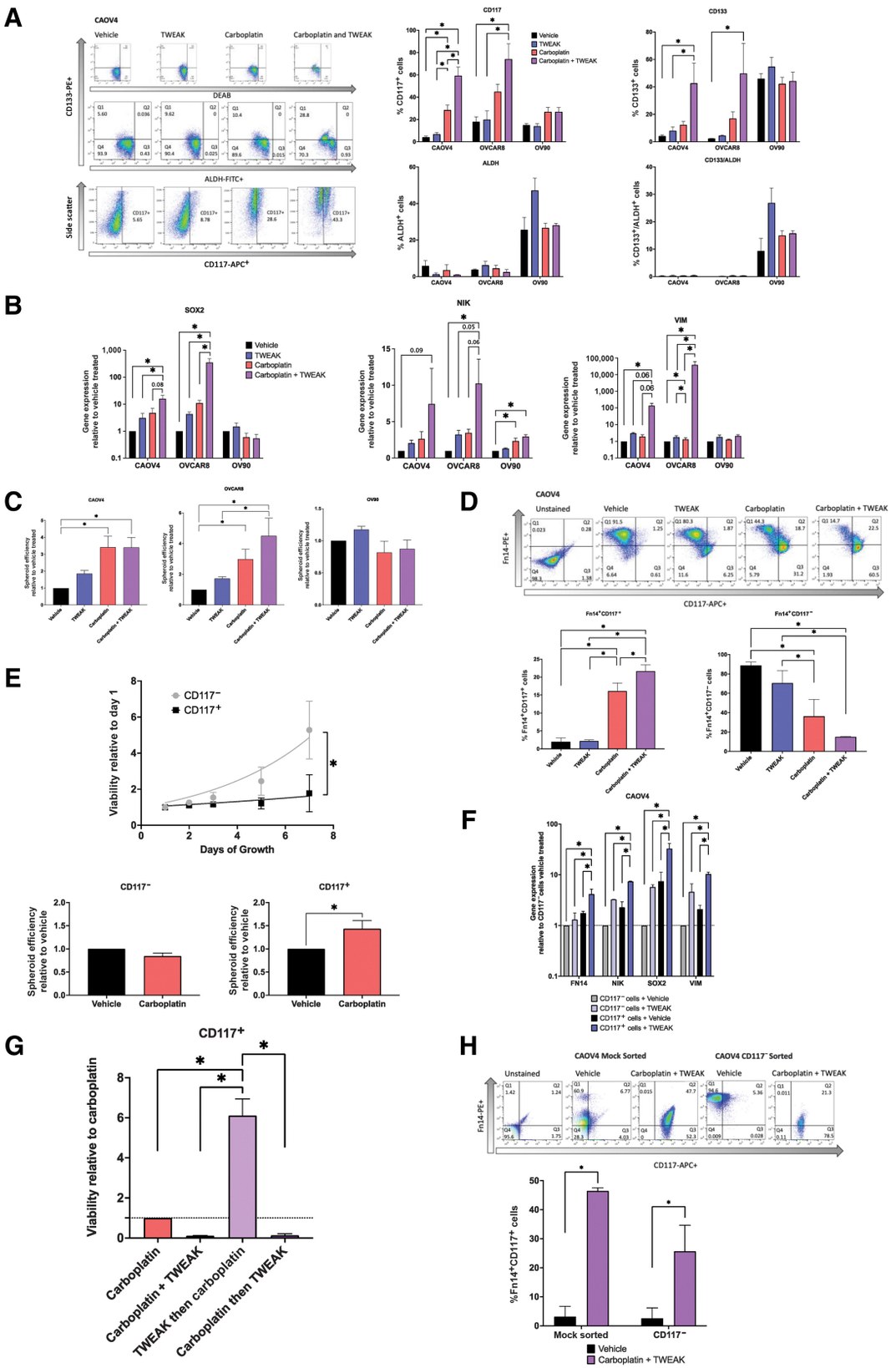
A
CAOV4
Vehicle
TWEAK
Carboplatin
Carboplatin and TWEAK
CD133-PE+
DEAB
ALDH-FITC+
Side scatter
CD117-APC+
CD117
% CD117+ cells
Vehicle
TWEAK
Carboplatin
Carboplatin + TWEAK
CD133
% CD133+ cells
ALDH
% ALDH+ cells
CD133/ALDH
% CD133+/ALDH+ cells
CAOV4
OVCAR8
OV90
B
SOX2
NIK
VIM
Gene expression relative to vehicle treated
C
Spheroid efficiency relative to vehicle treated
D
Fn14-PE+
CD117-APC+
Fn14+CD117+
Fn14+CD117−
% Fn14+CD117+ cells
% Fn14+CD117− cells
E
CD117−
CD117+
Viability relative to day 1
Days of Growth
Spheroid efficiency relative to vehicle
Vehicle
Carboplatin
F
Gene expression relative to CD117− cells vehicle treated
FN14
NIK
SOX2
VIM
CD117− cells + Vehicle
CD117− cells + TWEAK
CD117+ cells + Vehicle
CD117+ cells + TWEAK
G
Viability relative to carboplatin
Carboplatin
Carboplatin + TWEAK
TWEAK then carboplatin
Carboplatin then TWEAK
H
CAOV4 Mock Sorted
CAOV4 CD117− Sorted
Unstained
%Fn14+CD117+ cells
Mock sorted
CD117−

hydrogen peroxide. Slides were incubated with primary antibodies overnight at 4°C followed by an HRP-linked secondary for 1 hour at room temperature and processed using DAB (Supplementary Table S2). Four randomly selected, blinded images per slide were acquired with an Olympus BX51 with CellSens Standard software. Digital quantification of DAB staining was performed using ImageJ with a FIJI deconvolution package as described previously (9).

For IF, tumors were fixed, embedded, and antigen retrieval was done as above. Slides were blocked with 1% goat serum in PBS and then incubated with RelB-FITC primary antibody overnight (Supplementary Table S2). Slides were mounted with the Fluoroshield antifade medium with DAPI, and four randomly selected, blinded images per slide were acquired within 1 to 3 days with an Olympus BX63 with CellSens Standard software. Exposure time and beam intensity were kept consistent. Nuclear and cytosolic digital quantification of IF staining was performed blinded using automated imaging analysis with CellProfiler (22) and modeled with image set BBC014v1 (23). The Nuclear–cytosolic ratio was calculated as described previously (24).

Public database analysis

Public databases were queried as clarified (Supplementary Table S3).

Statistical analysis

Statistics were generated using Prism 9.3.1 with data acquired from at least three independent biological replicates. Results are presented as mean ± SEM. Significance was calculated using either Student *t* test for comparisons of two means or ANOVA for comparisons of three or more means with a *post hoc* test to identify differences between groups as described in figure legends. Differences between means are considered statistically significant at the 95% level ($P < 0.05$). Statistics were completed as described here or as otherwise noted in the figure legends.

Data availability

The data generated in this study are available upon request from the corresponding author.

Results

To identify factors that sufficiently activate NF-κB in ovarian cancer, we first exposed three different HGSOC ovarian cancer cell lines, including primary tumor-derived line OVCAR8, metastatic site-derived CAOV4, and ascites-derived OV90 (Supplementary Table S1; refs. 25, 26), each stably expressing an NF-κB luciferase reporter to increasing concentrations of known NF-κB inducers. We found consistently elevated signaling in response to TNFα and TWEAK across all three cell lines tested (**Fig. 1A**). TNFα-induced activation of classic NF-κB has been shown in several studies to contribute to ovarian cancer progression and metastasis (27–29); however, few studies to date have investigated the role of TWEAK in this disease (30, 31). To expand on these findings, we next performed an NF-κB DNA-binding assay to determine the relative abundance of activated NF-κB transcription factors in nuclear lysates collected after 2 and 24 hours of TWEAK stimulation. All three cell lines tested show significantly enhanced activation of both classic (p50 and p65) and alternative (p52 and RelB) NF-κB proteins after 24-hour stimulation relative to the vehicle; however, activation of RelB is highest across the three cell lines tested, relative to the other NF-κB subunits (**Fig. 1B**). To lend further support to these findings, we performed a western blot on nuclear and cytosolic lysates collected from ovarian cancer cell lines treated with TWEAK for 2 or 24 hours. TWEAK stimulation leads to strong nuclear localization of alternative NF-κB subunit factors p52 and RelB (**Fig. 1C**). RelA nuclear localization was minimally increased with TWEAK stimulation. Similar results were found in a primary cell line (VBCF004) derived from the ascites of an HGSOC patient (**Fig. 1D**). Together, these data suggest TWEAK is a strong inducer of alternative NF-κB activation that can also induce some classic NF-κB activity in ovarian cancer cells.

We next investigated the significance of TWEAK in tumor samples from ovarian cancer patients and mouse models of ovarian cancer. We found that soluble TWEAK in ascites derived from HGSOC patients with recurrent, chemoresistant disease had an average concentration of 4,241 pg/mL (288–1,4798 pg/mL) and, although lower, is analogous to the average IL6 concentration of 7,677 pg/mL (2,527–12,427 pg/mL; **Fig. 2A**). IL6 is a cytokine shown to be important and present at high levels in ovarian cancer progression and relapse (32, 33). These data suggest TWEAK is an appreciable component of the ovarian TME.

To establish TWEAK expression in clinical samples, we assessed *TWEAK* transcripts in tumor samples derived from HGSOC patients undergoing neoadjuvant chemotherapy (NACT; ref. 33). Post-NACT tumor samples had significantly higher levels of *TWEAK* mRNA relative to patient-matched pre-NACT tumor samples (**Fig. 2B**). These findings were confirmed using another

Figure 4.

TWEAK in combination with carboplatin enriches for CSCs and eliminates non-CSCs. **A,** Stem cell marker flow cytometry of HGSOC cells treated with vehicle, TWEAK (100 ng/mL), carboplatin (125 μmol/L), or TWEAK and carboplatin for 72 hours. Representative gating for CAOV4 (left), percent positive cells representing mean plus SD (right). One-way ANOVA, Tukey *post hoc* test ($n = 3$). **B,** qRT-PCR for select stemness genes in HGSOC cells with vehicle, TWEAK (100 ng/mL), carboplatin (125 μmol/L), or TWEAK and carboplatin for 72 hours represented relative to the vehicle. One-way ANOVA, Tukey *post hoc* test ($n = 3$). **C,** Spheroid efficiency of HGSOC cells treated with vehicle, TWEAK (100 ng/mL), carboplatin (125 μmol/L), or TWEAK and carboplatin for 4 days represented relative to vehicle. One-way ANOVA, Tukey *post hoc* test ($n = 4$). **D,** Flow cytometry analysis of CD117 expression on Fn14$^+$ cells treated with vehicle, TWEAK (100 ng/mL), carboplatin (125 μmol/L), or TWEAK and carboplatin for 72 hours. Representative gating (left) and percent positive cells representing mean plus SD (right). One-way ANOVA, Tukey *post hoc* test ($n = 3$). **E,** Viability of sorted OV90 CD117$^+$ or CD117$^-$ cells grown for 8 days normal media (top). Two-way repeated-measures ANOVA, Sidak *post hoc* test ($n = 4$). Spheroid efficiency of OV90 CD117$^+$ or CD117$^-$ cells treated with carboplatin (90 μmol/L) for 4 days represented relative to vehicle (bottom). Unpaired *t* test ($n = 4$). **F,** qRT-PCR of select genes for sorted CD117$^+$ or CD117$^-$ cells treated with vehicle or TWEAK (100 ng/mL) for 72 hours. One-way ANOVA, Tukey *post hoc* test ($n = 4$). **G,** Viability of CD117$^+$ sorted CAOV4 cells treated with either carboplatin (125 μmol/L), carboplatin and TWEAK (100 ng/mL), TWEAK then carboplatin, and carboplatin then TWEAK for 120 hours. One-way ANOVA, Tukey *post hoc* test ($n = 3$). **H,** Flow cytometry analysis of CD117 and Fn14 expression CAOV4 cells mock sorted or CD117$^-$ sorted cells treated with vehicle or TWEAK (100 ng/mL) and carboplatin (30 μmol/L) for two cycles of 7 days, where initial treatment is for 24 hours with subsequent 2-fold dilution with media. Representative gating (top) and percent Fn14$^+$CD117$^+$ cells representing mean plus SD. Two-way ANOVA, Sidak *post hoc* test ($n = 4$ mock, 5 CD117$^-$ sorted). Data represent mean and SEM. *, $P < 0.05$.

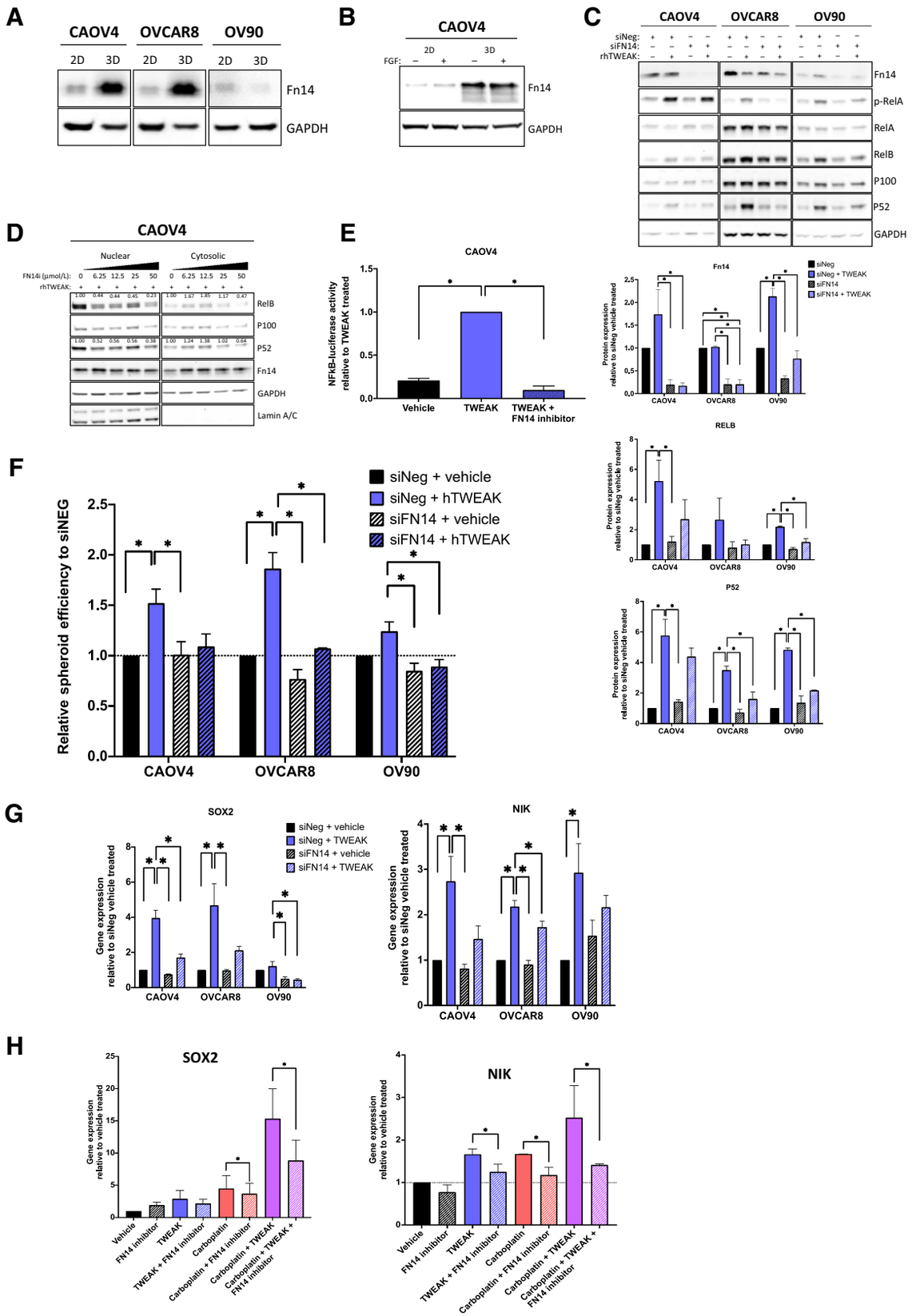
A
CAOV4
OVCAR8
OV90
2D
3D
Fn14
GAPDH
B
CAOV4
FGF:
Fn14
GAPDH
C
CAOV4
OVCAR8
OV90
siNeg:
siFN14:
rhTWEAK:
Fn14
p-RelA
RelA
RelB
P100
P52
GAPDH
D
CAOV4
Nuclear
Cytosolic
FN14i (μmol/L):
rhTWEAK:
RelB
P100
P52
Fn14
GAPDH
Lamin A/C
E
CAOV4
NFkB-luciferase activity relative to TWEAK treated
Vehicle
TWEAK
TWEAK + FN14 inhibitor
Fn14
siNeg
siNeg + TWEAK
siFN14
siFN14 + TWEAK
Protein expression relative to siNeg vehicle treated
RELB
P52
F
siNeg + vehicle
siNeg + hTWEAK
siFN14 + vehicle
siFN14 + hTWEAK
Relative spheroid efficiency to siNEG
CAOV4
OVCAR8
OV90
G
SOX2
NIK
siNeg + vehicle
siNeg + TWEAK
siFN14 + vehicle
siFN14 + TWEAK
Gene expression relative to siNeg vehicle treated
H
SOX2
NIK
Gene expression relative to vehicle treated
Vehicle
FN14 inhibitor
TWEAK
TWEAK + FN14 inhibitor
Carboplatin
Carboplatin + FN14 inhibitor
Carboplatin + TWEAK
Carboplatin + TWEAK + FN14 inhibitor

recently published data set (Supplementary Fig. S1A; method in Supplementary Table S3; ref. 34). Further analysis of these samples shows that *TWEAK* mRNA levels positively correlate with CSC marker *CD117*, and the epithelial-to-mesenchymal transition (EMT) markers, *ZEB1* and *CDH2* (N-cadherin). Conversely, *TWEAK* mRNA negatively correlates with epithelial marker genes *EPCAM* and *CDH1* (E-cadherin) and the proliferation marker *MKI67* (Ki-67; **Fig. 2C**).

Given its established role in tissue repair and its elevated expression post-NACT, we reasoned that TWEAK levels might be higher in cytotoxic chemotherapy-treated tumors relative to vehicle-treated tumors. Indeed, subcutaneous xenograft tumors resected from mice receiving three cycles of carboplatin chemotherapy exhibited higher levels of soluble TWEAK relative to mice receiving vehicle (**Fig. 2D**). Moreover, fixed tumors resected from chemotherapy-treated mice showed significantly higher expression of the TWEAK receptor, Fn14, relative to tumors from vehicle-treated mice (**Fig. 2D**). Altogether, these findings support the notion that TWEAK is present in the ovarian TME, that it correlates with the expression of stem and EMT genes, and that it is elevated after chemotherapy treatment.

Analysis of ovarian cancer data sets, including TCGA, revealed a significant decrease in progression-free and overall survival of HGSOC patients whose tumors have high expression of *TWEAK* transcripts (**Fig. 2E**; Supplementary Fig. S1B and S1C). Moreover, tumors from TCGA patients who had a recurrence had significantly higher levels of *TWEAK* transcripts relative to patients who remained tumor-free (**Fig. 2F**). Given the specificity of TWEAK for its receptor, Fn14 (35), we confirmed the elevated expression of *FN14* transcripts in ovarian cancer tissues relative to normal ovarian tissue (**Fig. 2G**). Data sets, including TCGA, further show that *FN14* expression is associated with a decrease in overall survival (Supplementary Fig. S1D). We confirmed that *TWEAK* and *FN14* were not comparatively high in normal ovarian tissues nor in our cell lines (Supplementary Fig. S1E and S1F). We then confirmed that Fn14 was present on ovarian cancer cells by flow cytometry (Supplementary Fig. S1G), and that *TWEAK* gene expression is not changed in ovarian cancer cells after carboplatin treatment (Supplementary Fig. S1H), suggesting TWEAK is produced from other cells in the TME.

We next conducted several experiments to examine the effects of TWEAK stimulation on tumor cells. Exogenous TWEAK stimulation for 72 hours had minimal effects on viability (Supplementary Fig. S2A) or proliferation as measured by Ki-67 staining (Supplementary Fig. S2B) or EdU incorporation (Supplementary Fig. S2C). Only the CAOV4 cell line exhibited a small but significant decrease in viability and proliferation when stimulated with TWEAK. Likewise, there was no significant effect on apoptosis when cells were treated with TWEAK relative to vehicle-treated cells as demonstrated by the TUNEL assay (Supplementary Fig. S2D) and caspase activity assay (Supplementary Fig. S2E). By contrast, carboplatin significantly induced apoptosis in these cells. Given these findings and its ability to activate alternative NF-κB signaling, its correlation with stem cell marker gene expression, and its enrichment with chemotherapy, we hypothesized that TWEAK may contribute to phenotypes associated with CSCs.

We have previously shown that spheroid formation was at least partially dependent on NF-κB transcription factors (18), so we tested whether TWEAK stimulation enhances the ability of ovarian cancer cells to form spheroids and asymmetrically divide. Because these processes largely depend on the activation of EMT genes and stem cell transcription factors that support long-term self-renewal and asymmetric division, we first examined transcript levels of relevant genes after TWEAK stimulation (**Fig. 3A** and **B**). TWEAK induced a significant increase in the expression of NF-κB inducing kinase (*NIK*), a critical kinase in the alternative NF-κB signaling pathway, in all cells. Expression of the EMT gene Vimentin (*VIM*) also significantly increased in all cell lines tested, whereas *ZEB1* increased in CAOV4 and OVCAR8. The epithelial marker gene *CDH1* decreased in OVCAR8 and VBCF004. There was no significant difference in *OCT4* or *NANOG* expression with TWEAK stimulation in any of the cell lines; however, *SOX2* was upregulated in CAOV4 and OVCAR8.

We then examined spheroid formation and asymmetric division. Relative to the vehicle, TWEAK significantly enhanced spheroid formation efficiency in CAOV4 and OVCAR8 cells, but not in OV90 cells (**Fig. 3C**). TWEAK treatment also promoted spheroid formation in the primary cells (**Fig. 3D**). There was a significant decrease in F-actin staining, a factor that increases during cell differentiation (**Fig. 3E**; refs. 36, 37) and a corresponding decrease in the symmetric division after TWEAK stimulation relative to vehicle (**Fig. 3F**). These data indicate that TWEAK can induce expression of genes associated with stemness and/or EMT and can promote spheroid formation and asymmetric division in a variety of ovarian cancer cells.

To better characterize the effects of TWEAK–Fn14 signaling on CSC populations, we examined ovarian cancer cells expressing known markers of ovarian CSCs (CD117, CD133, and ALDH) with TWEAK stimulation in the presence or absence of chemotherapy. Relative to vehicle, there was no significant difference in the percentage of cells expressing traditional CSC markers when stimulated with TWEAK, with the exception of OV90, which showed an increase of cells with ALDH activity (**Fig. 4A**). As expected, with carboplatin treatment, there was a significant enrichment of $CD117^+$ and/or $CD133^+$ cells in the CAOV4 and

Figure 5.

TWEAK receptor Fn14 is required for TWEAK-mediated stem-like features. **A,** Western blot for Fn14 from cells grown in standard adherent conditions or in spheroid conditions. **B,** Western blot for Fn14 from cells grown in standard monolayer conditions or in spheroid suspension conditions with or without FGF. **C,** Western blot of Fn14 and NF-κB proteins in siNeg or siFN14 HGSOC cells treated with vehicle or TWEAK (100 ng/mL) for 72 hours. Representative image (top) and quantification of band intensities (bottom). One-way ANOVA, Tukey *post hoc* test ($n = 3$). **D,** Nuclear and cytosolic western blots for indicated proteins in CAOV4 cells treated with TWEAK (100 ng/mL), or TWEAK plus FN14 inhibitor (L542-0366, 6.25–50 μmol/L). Quantification values normalized to Lamin A/C for nuclear fraction and GAPDH for a cytosolic fraction. **E,** Luciferase reporter assay showing NF-κB activity is lost in response to TWEAK (100 ng/mL) plus FN14i (L542-0366, 50 μmol/L) in CAOV4 cells ($n = 4$). **F,** Spheroid efficiency of siNeg or siFN14 HGSOC cells treated with vehicle or TWEAK (100 ng/mL) for 4 days, represented relative to vehicle. One-way ANOVA, Tukey *post hoc* test ($n = 4$). **G,** qRT-PCR for SOX2 or NIK in siNeg or siFN14 HGSOC cells treated with TWEAK (100 ng/mL) for 48 hours, relative to vehicle. One-way ANOVA, Tukey *post hoc* test ($n = 3$). **H,** qRT-PCR for SOX2 or NIK in CAOV4 cells treated with FN14 inhibitor (L542–0366, 50 μmol/L) for 72 hours in combination with vehicle, TWEAK (100 ng/mL), carboplatin (125 μmol/L), or TWEAK and carboplatin conditions. Unpaired *t* test for condition versus condition plus FN14 inhibitor ($n = 3$). Data represent mean and SEM. * $P < 0.05$.

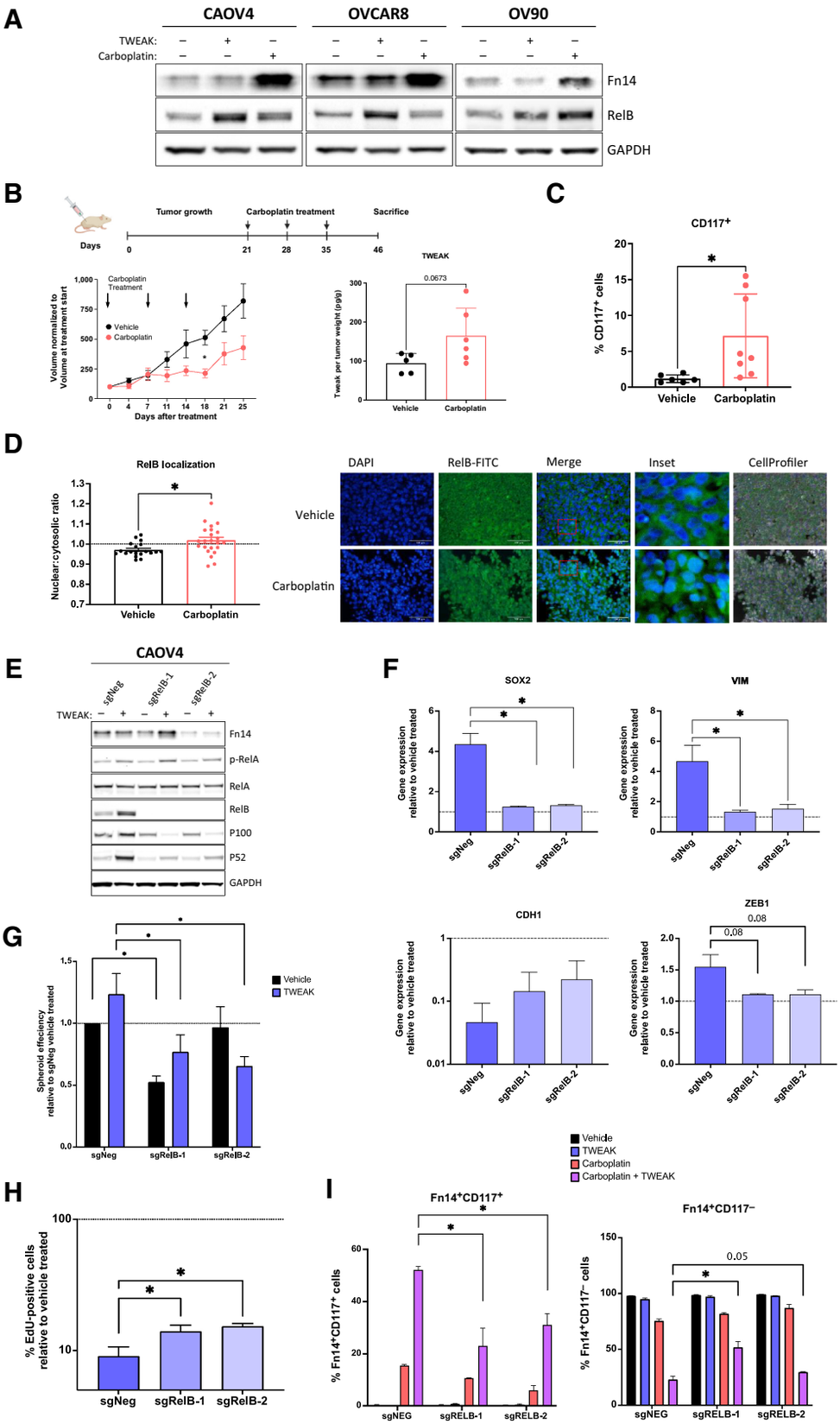
A
CAOV4
OVCAR8
OV90
TWEAK:
Carboplatin:
Fn14
RelB
GAPDH
B
Tumor growth
Carboplatin treatment
Sacrifice
Days
0
21
28
35
46
Carboplatin Treatment
Vehicle
Carboplatin
Volume normalized to Volume at treatment start
Days after treatment
TWEAK
0.0673
Tweak per tumor weight (pg/g)
Vehicle
Carboplatin
C
CD117+
% CD117+ cells
Vehicle
Carboplatin
D
RelB localization
Nuclear:cytosolic ratio
Vehicle
Carboplatin
DAPI
RelB-FITC
Merge
Inset
CellProfiler
E
CAOV4
sgNeg
sgRelB-1
sgRelB-2
TWEAK:
Fn14
p-RelA
RelA
RelB
P100
P52
GAPDH
F
SOX2
VIM
CDH1
ZEB1
0.08
Gene expression relative to vehicle treated
sgNeg
sgRelB-1
sgRelB-2
G
Spheroid efficiency relative to sgNeg vehicle treated
Vehicle
TWEAK
H
% EdU-positive cells relative to vehicle treated
I
Fn14+CD117+
Fn14+CD117−
% Fn14+CD117+ cells
% Fn14+CD117− cells
0.05
sgNEG
sgRELB-1
sgRELB-2
Vehicle
TWEAK
Carboplatin
Carboplatin + TWEAK

OVCAR8 cell lines. In agreement with our previous findings, we observe that $CD133^+ALDH^+$ double-positive cells are enriched in OV90 cells after chemotherapy treatment (9). We have shown in other studies that CAOV4 and OVCAR8 do not express sufficient $CD133^+ALDH^+$ cells (9, 25). Interestingly, carboplatin combined with TWEAK led to the largest enrichment of CD117 and CD133 expressing cells in two of the three lines tested. Notably, the combination treatment led to an almost complete elimination of $CD117^-$ cells, as $CD117^+$ cells made up 65% to 85% of the surviving population in CAOV4 and OVCAR8 cells (**Fig. 4A**). We examined gene-expression changes in cells undergoing these treatments and found that although TWEAK stimulation alone enhances expression of *SOX2*, *NIK*, and *VIM* genes, combining it with chemotherapy leads to the largest increase in expression of these genes (**Fig. 4B**). This treatment combination similarly led to the greatest increase in spheroid development (**Fig. 4C**), in agreement with other studies (38–41), presumably due to enrichment of CSCs. Interestingly, OV90 cells do not respond to TWEAK as strongly as the other cell lines, and this is likely due to the high endogenous levels of SOX2 previously established in this line (9) and the relatively low level of Fn14 expression, we discover in this study. Taken together, these data suggest that TWEAK enhances either the development of new CSCs during chemotherapy or improves the ability of carboplatin to eliminate non-CSCs. Either scenario would lead to an enrichment of CSCs after chemotherapy.

To further investigate this, we assessed changes in the percentage of cells expressing both the Fn14 receptor ($Fn14^+$) and CD117 ($CD117^+$) under these same treatment conditions. Although there is a significant increase in the percentage of $Fn14^+CD117^+$ cells with TWEAK in combination with carboplatin relative to all other treatments, there is a significant decrease in the percentage of $Fn14^+CD117^-$ cells under this treatment regimen (**Fig. 4D**). These findings suggest that the effects of TWEAK on non-CSCs ($CD117^-$) are different from those on CSCs ($CD117^+$). As further validation of CD117 as an ovarian cancer CSC marker, we performed column separation of $CD117^+$ and $CD117^-$ cells and assessed growth rates and spheroid chemosensitivity. $CD117^+$ cells grew significantly more slowly when compared with $CD117^-$ cells, and $CD117^+$ spheroids were chemoresistant to carboplatin treatment, whereas $CD117^-$ spheroids were somewhat more chemosensitive (**Fig. 4E**). To explore the possibility that TWEAK could act differently on non-CSCs and CSCs, we performed FACS on $CD117^+$ and $CD117^-$ cells and subsequently treated with TWEAK to evaluate changes in gene expression relative to vehicle. TWEAK treatment of $CD117^-$ cells enhances expression of *FN14*, *NIK*, *SOX2*, and *VIM* genes relative to vehicle-treated $CD117^-$ cells (**Fig. 4F**). The levels of gene expression in $CD117^-$ cells treated with TWEAK are comparable to those endogenously expressed in vehicle-treated $CD117^+$ cells. However, stimulation of $CD117^+$ cells with TWEAK led to the highest expression of these genes, relative to vehicle-treated $CD117^+$ cells.

To evaluate TWEAK-induced chemoresistance of $CD117^+$ cells associated with these gene changes, we compared different delivery times of TWEAK treatment in a chemosensitivity assay (**Fig. 4G**). We found that $CD117^+$ cells treated with TWEAK before the introduction of carboplatin had a 6-fold survival advantage, when compared with $CD117^+$ carboplatin-treated cells, $CD117^+$ cells treated with carboplatin and TWEAK at the same time, and $CD117^+$ cells treated with TWEAK after carboplatin treatment. This suggests that TWEAK-induced gene changes can confer chemoresistance on $CD117^+$ cells. To evaluate whether TWEAK and chemotherapy can promote the expression of CD117 on $CD117^-$ cells, we treated either mock-sorted cells or $CD117^-$ sorted cells with two sequential treatments of serum concentration of carboplatin and TWEAK over 14 days, as we have done previously (9). Mock-sorted cells recapitulated our findings in **Fig. 4D** showing a significant increase in the percentage of $Fn14^+CD117^+$ cells when treated with TWEAK in combination with carboplatin (**Fig. 4H**). $CD117^-$ sorted cells treated with TWEAK in combination with carboplatin significantly upregulated CD117 relative to vehicle-treated cells. These experiments strongly support the idea that TWEAK acts on $CD117^+$ cells to enhance chemoresistance and, when combined with chemotherapy, enhances the development of $CD117^+$ cells from $CD117^-$ cells, both of which would facilitate the survival of CSCs during chemotherapy.

We next evaluated the specificity of TWEAK–Fn14-dependent differences in gene expression and spheroid formation. Expression of the Fn14 receptor is dramatically increased in CSC-enriching 3-D cultures, relative to 2-D monolayer cultures in CAOV4 and OVCAR8 cells (**Fig. 5A**). We verified that this enriched expression was not due to fibroblast growth factor, a component of 3-D culture media (**Fig. 5B**). Knockdown of the receptor using siRNA or FN14 inhibitor (L542-0366) eliminated the TWEAK-induced NF-κB activation (**Fig. 5C–E**), spheroid formation (**Fig. 5F**), and *SOX2* and *NIK* expression (**Fig. 5G**), implicating TWEAK–Fn14 as a vital upstream contributor to the CSC phenotype observed in ovarian cancer cells. We also confirmed that the upregulation of *SOX2* and *NIK,* which was most enhanced with a combination of carboplatin and TWEAK, was lost when the treatment included an FN14 inhibitor (**Fig. 5H**).

We have previously shown that RelB expression is enhanced in ovarian cancer cells after chemotherapy or when grown in 3-D conditions (18). In this study, we discovered that Fn14 expression is also enhanced with chemotherapy and 3-D culture conditions (**Fig. 5A**

Figure 6.

RelB mediates TWEAK–Fn14-dependent enrichment of CSCs and elimination of non-CSCs. **A,** Western blot for Fn14 and RelB from cells treated with vehicle, TWEAK, or carboplatin for 72 hours. **B–C,** Subcutaneous tumors were generated in nude mice using OV90 cells. Tumors were allowed to grow for 21 days followed by 3 cycles of carboplatin (50 mg/kg) or vehicle and resected 12 days after the final carboplatin treatment. **B,** Experimental design created with BioRender.com (left). Tumor volume was measured twice weekly and graphed normalized to the volume at treatment start (center). Two-way ANOVA, Tukey *post hoc* test ($n = 6$). TWEAK concentration per tumor weight measured using ELISA (right). Unpaired *t* test ($n = 6$). **C,** Flow cytometry analysis of CD117 expression on excised tumors following dissociation into single-cell suspension. Unpaired *t* test ($n = 8$). **D,** Fixed tumor fractions were histologically stained for nuclei (DAPI) and RelB. Representative images (left) and nuclear relative to cytosolic RelB were quantified per field using CellProfiler (right). Unpaired *t* test ($n = 3$). **E,** Western blot of NF-κB proteins in CAOV4-RelB knockout (KO) lines with TWEAK treatment (100 ng/mL) for 48 hours. **F,** qRT-PCR for select genes in CAOV4-RelB KO lines treated with TWEAK (100 ng/mL) for 48 hours, relative to vehicle. One-way ANOVA, Tukey *post hoc* test ($n = 3$). **G,** Spheroid efficiency of CAOV4-RelB KO lines treated with TWEAK (100 ng/mL) for 7 days, relative to vehicle. Two-way ANOVA, Tukey *post hoc* test ($n = 6$). **H,** EdU incorporation pulse-chase assay of CAOV4-RelB KO lines treated with TWEAK (100 ng/mL) for 60 hours, relative to vehicle. One-way ANOVA, Tukey *post hoc* test ($n = 6$). **I,** Flow cytometry of CD117 expression on $Fn14^+$ CAOV4-RelB KO lines treated with TWEAK (100 ng/mL), carboplatin (125 μmol/L), or TWEAK and carboplatin for 72 hours, represented relative to vehicle as mean plus SD. One-way ANOVA, Tukey *post hoc* test ($n = 3$). Data, mean and SEM. *, $P < 0.05$.

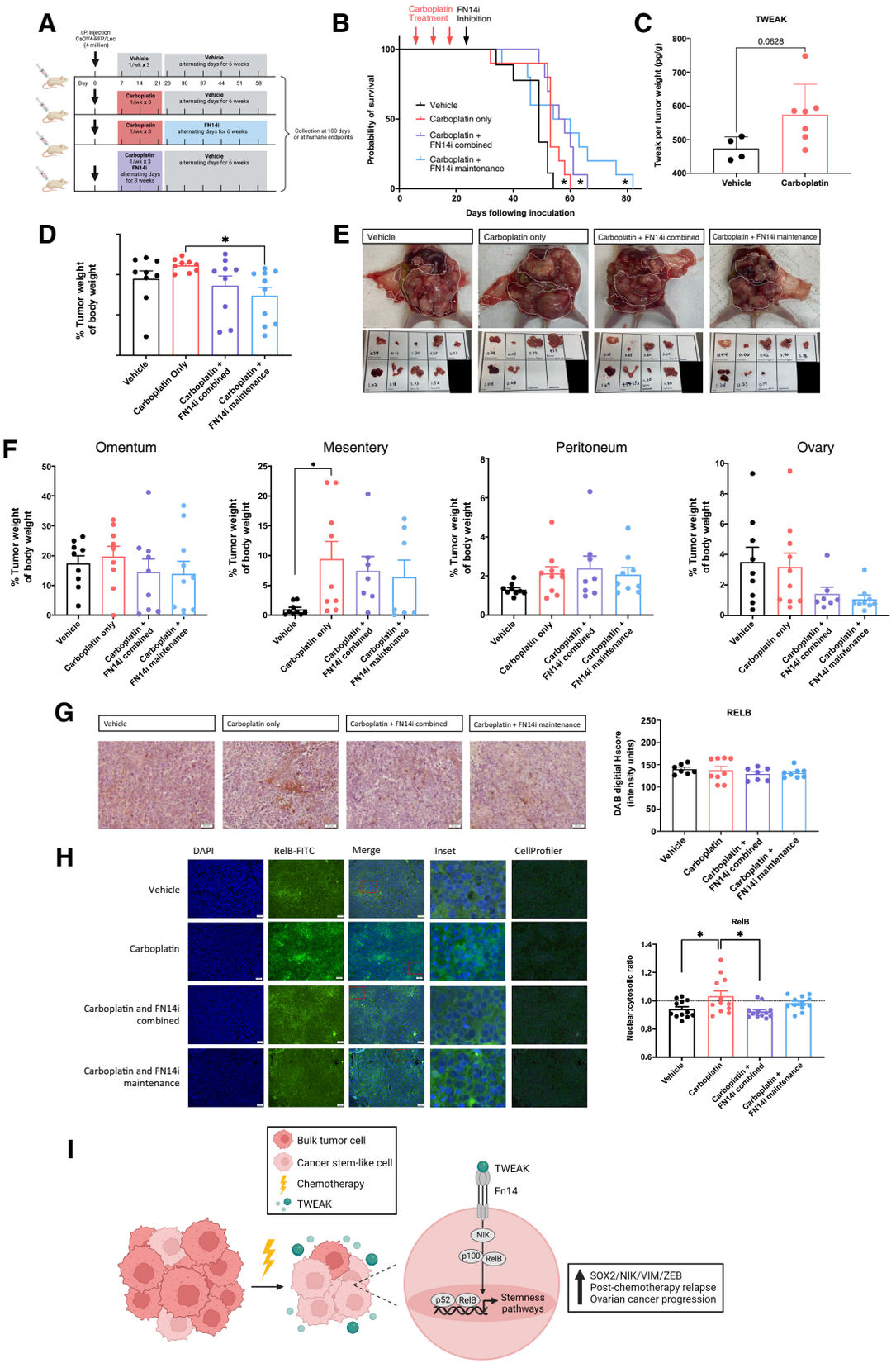
A
I.P. Injection CaOV4-RFP/Luc (4 million)
Vehicle 1/wk x 3
Vehicle alternating days for 6 weeks
Day 0 7 14 21 23 30 37 44 51 58
Carboplatin 1/wk x 3
FN14i alternating days for 6 weeks
Carboplatin 1/wk x 3 FN14i alternating days for 3 weeks
Collection at 100 days or at humane endpoints
B
Carboplatin Treatment
FN14i Inhibition
Probability of survival
Vehicle
Carboplatin only
Carboplatin + FN14i combined
Carboplatin + FN14i maintenance
Days following inoculation
C
TWEAK
0.0628
Tweak per tumor weight (pg/g)
Vehicle
Carboplatin
D
% Tumor weight of body weight
Vehicle
Carboplatin Only
Carboplatin + FN14i combined
Carboplatin + FN14i maintenance
E
Vehicle
Carboplatin only
Carboplatin + FN14i combined
Carboplatin + FN14i maintenance
F
Omentum
Mesentery
Peritoneum
Ovary
% Tumor weight of body weight
G
RELB
DAB digital Hscore (intensity units)
H
DAPI
RelB-FITC
Merge
Inset
CellProfiler
Vehicle
Carboplatin
Carboplatin and FN14i combined
Carboplatin and FN14i maintenance
RelB
Nuclear:cytosolic ratio
I
Bulk tumor cell
Cancer stem-like cell
Chemotherapy
TWEAK
Fn14
NIK
p100
RelB
p52
Stemness pathways
SOX2/NIK/VIM/ZEB
Post-chemotherapy relapse
Ovarian cancer progression

and **6A**). Moreover, TWEAK treatment leads to higher expression of RelB relative to carboplatin (**Fig. 6A**). To assess the delayed effect of TWEAK on downstream targets like CSC features and RelB in post-chemotherapy tumors, we resected xenograft tumors 12 days after three cycles of carboplatin were completed in a relapsing subcutaneous mouse model, in contrast to 5 days after chemotherapy presented in **Fig. 2G**. Soluble TWEAK remained high in chemotherapy-treated mice relative to mice receiving vehicle (**Fig. 6B**). As expected, there was a significant enrichment for $CD117^+$ expressing cells (**Fig. 6C**), as well as RelB nuclear localization following chemotherapy (**Fig. 6D**). To determine if the TWEAK-induced CSC features are dependent on RelB, we used CRISPR-Cas9 editing technology to knock out the RelB transcription factor in CAOV4 cells (**Fig. 6E**). Loss of RelB prevented the upregulation of *SOX2*, *VIM*, and *ZEB1* genes induced by TWEAK (**Fig. 6F**). Moreover, the downregulation of *CDH1* induced by TWEAK was partially rescued with knockout of RelB. Loss of RelB also diminished TWEAK-induced spheroid forming ability (**Fig. 6G**) and asymmetric division (**Fig. 6H**). The percentage of $Fn14^+CD117^+$ cells surviving carboplatin alone and carboplatin combined with TWEAK was significantly hampered with knock out of RelB (**Fig. 6I**). Similarly, loss of RelB led to a significant enrichment in the percentage of $Fn14^+CD117^-$ cells, indicating the diverse effects of TWEAK on $CD117^+$ and $CD117^-$ cells are at least partially dependent on RelB. Thus, TWEAK may be a promising upstream target for inhibiting NF-κB–dependent phenotypes, such as chemoresistance in CSCs.

We next tested whether inhibiting TWEAK activity *in vivo* could prolong survival in an i.p. xenograft mouse model of ovarian cancer. Given that TWEAK is likely secreted by stromal cells (35, 42), we first verified that mouse TWEAK is structurally homologous to human TWEAK (Supplementary Fig. S3A and S3B), can sufficiently activate NF-κB (Supplementary Fig. S3C and S3D), and induce spheroid formation (Supplementary Fig. S3E) in human ovarian cancer cells, can induce expression of *SOX2* and *NIK* as observed with human TWEAK (Supplementary Fig. S3F), and that these phenotypes are dependent on the human Fn14 receptor (Supplementary Fig. S3D–S3F).

Because TWEAK levels appear to be highest with chemotherapy administration, we assessed whether inhibiting TWEAK–Fn14 signaling in combination with carboplatin chemotherapy or as maintenance therapy after the completion of 3 cycles of carboplatin would prolong overall survival in an i.p. model (**Fig. 7A**). Administration of the FN14 inhibitor L542-0366, in combination with carboplatin, significantly prolonged overall survival (**Fig. 7B**). The longest overall survival was observed when the L542-0366 was given as a maintenance therapy following three cycles of carboplatin chemotherapy (**Fig. 7B**). Consistent with our subcutaneous xenograft tumor model, TWEAK was enriched in chemotherapy-treated IP tumors relative to vehicle (**Fig. 7C**). Tumor weights at necropsy were significantly lower for mice treated with L542-0366 as a maintenance, relative to carboplatin alone (**Fig. 7D** and **E**). Furthermore, FN14 inhibition leads to lower tumor burden at the ovary (**Fig. 7F**). IHC analysis of resected tumors showed that the overall levels of RelB at necropsy are not significantly different among any of the treatment groups (**Fig. 7G**); however, blinded automated imaging analysis with CellProfiler as previously described (22–24) demonstrates reduced nuclear localization of RelB in L524-0366-treated tumors, relative to vehicle or chemotherapy alone (**Fig. 7H**). These data indicate that inhibiting TWEAK–Fn14 signaling following standard 3-cycle chemotherapy provides a survival benefit in mice. Our *in vitro* data suggest this may be due to the ability of TWEAK to promote expression of stemness genes and corresponding phenotypes in CSCs via alternative pathway NF-κB activity during chemotherapy. Thus, blocking the TWEAK–Fn14–NF-κB signaling cascade should be further explored as a potential clinical approach to prolong remission in ovarian cancer patients.

Discussion

In addition to tumor cells, the ovarian TME is characterized by a variety of nontumor cells including tumor-associated macrophages, cancer-associated adipocytes, and cancer-associated fibroblasts, all of which secrete cytokines that can activate NF-κB and/or stemness signaling pathways in cancer cells (14, 43). Emerging studies in ovarian cancer implicate the TME in inducing stemness through the secretion of cytokines that alter signaling pathways and/or epigenetic patterns (32, 44). NF-κB, a master regulator of diverse cellular processes, is persistently activated in ovarian cancer and is associated with a poor prognosis (12, 19, 45). We previously identified a novel role for the alternative NF-κB transcription factor subunit, RelB, in maintaining ovarian CSCs with low proliferative potential, tumor initiation capacity, and chemotherapy resistance (18). Given its robust activation by various stimuli, in this study, we sought to identify consistent inducers of alternative NF-κB that may serve as promising targets for eliminating CSCs and preventing recurrence in ovarian cancer.

We discovered that TWEAK is a strong inducer of the alternative NF-κB pathway in HGSOC cells and is enriched in tumors following chemotherapy. A previous study showed that TWEAK–Fn14 signaling contributes to ovarian cancer metastasis via NF-κB-mediated upregulation of vascular endothelial growth factor (VEGF; ref. 30). This study focused on the role of classic NF-κB as a downstream effector of TWEAK–Fn14 signaling and did not investigate alternative NF-κB mechanisms. Although TWEAK can activate both classic and alternative NF-κB pathways, activation of the alternative pathway is more long term and may be restricted to specific cell types (35, 46–48). Our findings suggest TWEAK is a

Figure 7.

A small-molecule inhibitor of Fn14, as a maintenance therapy following chemotherapy, inhibits RelB activation and significantly slows ovarian cancer relapse. **A,** Experimental design created with BioRender.com. **B,** Kaplan–Meier survival of intraperitoneal xenograft tumors with CAOV4 cells treated with either vehicle, carboplatin (50 mg/kg), carboplatin and FN14i (L542-0366, 9 mg/kg) combined, or carboplatin followed by FN14i maintenance. Log-rank test ($n = 10$). **C,** TWEAK concentration per tumor weight. Unpaired *t* test ($n = 4$ vehicle, $n = 7$ treatment). **D,** Tumors were resected and weighed relative to body weight. One-way ANOVA, Tukey *post hoc* test. **E,** Representative images of tumors from different treatment groups at necropsy. **F,** Tumors were resected and weighed by organ, represented relative to body weight. One-way ANOVA, Tukey *post hoc* test ($n = 10$). **G,** Tumors were resected, fixed, and histologically stained RelB-DAB. Representative images (left) and quantification using ImageJ (right). One-way ANOVA, Tukey *post hoc* test ($n = 10$). Data represent mean and SEM. *, $P < 0.05$. **H,** Fixed tumor fractions were histologically stained for nuclei (DAPI) and RelB. Representative images (left) and nuclear relative to cytosolic RelB were quantified per field using CellProfiler (right). One-way ANOVA, Tukey *post hoc* test ($n = 3$). Data represent mean and SEM. * $P < 0.05$. **I,** Proposed mechanism created with BioRender.com to illustrate TWEAK–Fn14–RelB signaling supports post-chemotherapy ovarian cancer progression.

strong inducer of alternative NF-κB in ovarian cancer cells and promotes a stem-like phenotype. Interestingly, activation of either classic or alternative NF-κB by TWEAK can provoke contrasting phenotypes. For example, TWEAK-mediated activation of classic NF-κB leads to myoblast proliferation and suppression of myogenesis in muscle regeneration, whereas TWEAK-dependent activation of alternative NF-κB leads to myogenesis and suppression of myoblast proliferation (46). These findings are intriguing given our previous work in ovarian cancer showing that classic NF-κB signaling supports a proliferative phenotype, whereas alternative NF-κB supports a quiescent phenotype (18). Although the current study focuses on alternative NF-κB pathway-dependent processes promoted by TWEAK, future studies to unravel features facilitated by classic NF-κB would be worthwhile and may uncover a novel mechanism for maintaining heterogeneity in ovarian cancer. Although activation of NF-κB transcription factors is the most common effector of TWEAK–Fn14 signaling, other pathways including ERK, JNK, and PI3K/AKT have been shown to be induced by TWEAK in specific cell types, which together may affect ovarian cancer biology (35, 49, 50).

TWEAK is a cytokine of the TNF superfamily and its activity is mediated by binding, with high specificity, to its receptor, a type I transmembrane protein known as Fn14 (49–51). TWEAK and Fn14 are normally expressed at low levels in healthy tissues but can be upregulated during tissue injury, for example, in response to IFNγ (52–54). Transient TWEAK–Fn14 signaling is critical for efficient wound repair; however, constitutive expression of Fn14 is implicated in several diseases including cardiovascular disease, rheumatoid arthritis, and cancer (52, 53, 55). Our results show an upregulation of Fn14 on ovarian tumor cells following chemotherapy *in vitro* and *in vivo*. TWEAK is primarily secreted by macrophages and stromal cells (56–60), and given the tissue remodeling activities that underscore tumor formation and responses to cytotoxic treatments, it is conceivable that TWEAK is elevated in tumors and may be increased further following chemotherapy.

Our findings indicate that TWEAK–Fn14 signaling has diverse effects on subpopulations of ovarian cancer cells. Given that CD117 expression is a marker of chemoresistant CSCs (9, 61), we examined the effects of TWEAK on $CD117^+$ and $CD117^-$ cells. TWEAK–Fn14 signaling in $CD117^-$ bulk tumor cells appears to sensitize them to carboplatin chemotherapy as the percentage of $CD117^-$ cells decreases when TWEAK is combined with carboplatin. These findings are in agreement with previous studies showing that Fn14 expression sensitizes ovarian cancer cells to chemotherapy, although this study did not examine CSCs nor the role of TWEAK in this process (31). Conversely, we found that the percentage of $CD117^+$ cells increases with TWEAK and carboplatin treatment. Moreover, TWEAK stimulation of $CD117^+$ cells induces the highest expression of stemness genes, thus enhancing their CSC characteristics including their ability to survive in the presence of chemotherapy, and likely their ability to initiate relapse. Interestingly, TWEAK stimulation during carboplatin treatment of $CD117^-$ cells induced CD117 expression, suggesting a possible reprogramming of non-CSCs into CSCs in the presence of TWEAK. Our results align with several studies that implicate TWEAK in inhibiting differentiation, inducing EMT, and maintaining stemness in a variety of tissue types (52, 62–65).

Given the enrichment of TWEAK with chemotherapy and its ability to enhance CSC features, we propose that the TWEAK–Fn14–RelB signaling axis contributes to CSC development, thereby enhancing relapse potential in ovarian cancer (**Fig. 7I**). We show that a maintenance therapy inhibiting TWEAK signaling following carboplatin administration significantly prolonged survival in a mouse model of ovarian cancer. Our *in vitro* studies suggest this may be at least partially due to the inhibition of alternative NF-κB signaling, although we cannot rule out the involvement of other TWEAK signaling pathways. Future studies investigating the regulation of TWEAK in the ovarian TME may enable the development of new therapeutic approaches for preventing tumor recurrence in ovarian cancer.

Authors' Disclosures

B.G. Bitler reports grants from NCI/NIH, ACS, and DOD during the conduct of the study; other support from Onconic Therapeutics outside the submitted work. C.D. House reports grants from NCI and National Institute on Minority Health and Health Disparities during the conduct of the study. No disclosures were reported by the other authors.

Authors' Contributions

R. Holmberg: Conceptualization, data curation, formal analysis, validation, investigation, visualization, methodology, writing–original draft, writing–review and editing. **M. Robinson:** Conceptualization, data curation, formal analysis, validation, investigation, visualization, methodology, writing–original draft, writing–review and editing. **S.F. Gilbert:** Formal analysis, validation, investigation, visualization, methodology, project administration, writing–review and editing. **O. Lujano-Olazaba:** Formal analysis, validation, investigation, methodology, writing–review and editing. **J.A. Waters:** Formal analysis, validation, investigation, methodology. **E. Kogan:** Data curation, formal analysis. **C.L.R. Velasquez:** Validation, investigation. **D. Stevenson:** Validation, investigation. **L.S. Cruz:** Formal analysis, validation, investigation. **L.J. Alexander:** Validation, investigation. **J. Lara:** Formal analysis, validation, investigation. **E.M. Mu:** Validation, investigation. **J.R. Camillo:** Validation, investigation. **B.G. Bitler:** Resources, data curation, investigation, writing–review and editing. **T. Huxford:** Conceptualization, supervision, writing–review and editing. **C.D. House:** Conceptualization, resources, formal analysis, supervision, funding acquisition, validation, methodology, writing–original draft, project administration, writing–review and editing.

Acknowledgments

This work was funded by the National Institute on Minority Health and Health Disparities at the NIH under award number U54MD012397. This work was also supported by the NCI at the NIH under award numbers R00 CA20472703 and R01CA260281, and by the SDSU/UCSD Cancer Partnership funded by the National Cancer Institute at the NIH under award numbers U54CA132384 (SDSU) and U54CA132379 (UC San Diego). R. Holmberg was supported by the Arne N. Wick Predoctoral Fellowship from the California Metabolic Research Foundation. We thank Dr. Christina M. Annunziata and the National Cancer Institute for the kind gift of clinical ascites samples, Benjamin Canter of the SDSU FACS core facility for his excellent assistance with flow cytometry experiments, Larkin Slater of the SDSU vivarium for her assistance with mouse studies, and Natalie Gude for her assistance with histology studies.

The publication costs of this article were defrayed in part by the payment of publication fees. Therefore, and solely to indicate this fact, this article is hereby marked "advertisement" in accordance with 18 USC section 1734.

Note

Supplementary data for this article are available at Molecular Cancer Research Online (http://mcr.aacrjournals.org/).

Received June 17, 2022; revised September 12, 2022; accepted October 6, 2022; published first October 10, 2022.

References

1. Siegel RL, Miller KD, Jemal A. Cancer statistics, 2020. CA Cancer J Clin 2020;70:7–30.
2. Matulonis UA, Sood AK, Fallowfield L, Howitt BE, Sehouli J, Karlan BY. Ovarian cancer. Nat Rev Dis Primers 2016;2:16061.
3. Burgos-Ojeda D, Rueda BR, Buckanovich RJ. Ovarian cancer stem cell markers: prognostic and therapeutic implications. Cancer Lett 2012;322:1–7.
4. Zhang S, Balch C, Chan MW, Lai HC, Matei D, Schilder JM, et al. Identification and characterization of ovarian cancer-initiating cells from primary human tumors. Cancer Res 2008;68:4311–20.
5. Foster R, Buckanovich RJ, Rueda BR. Ovarian cancer stem cells: working towards the root of stemness. Cancer Lett 2013;338:147–57.
6. Terraneo N, Jacob F, Dubrovska A, Grünberg J. Novel therapeutic strategies for ovarian cancer stem cells. Front Oncol 2020;10:319.
7. Harrington BS, Ozaki MK, Caminear MW, Hernandez LF, Jordan E, Kalinowski NJ, et al. Drugs targeting tumor-initiating cells prolong survival in a post-surgery, post-chemotherapy ovarian cancer relapse model. Cancers (Basel) 2020;12:1645.
8. Hatina J, Boesch M, Sopper S, Kripnerova M, Wolf D, Reimer D, et al. Ovarian cancer stem cell heterogeneity. Adv Exp Med Biol 2019;1139:201–21.
9. Robinson M, Gilbert SF, Waters JA, Lujano-Olazaba O, Lara J, Alexander LJ, et al. Characterization of SOX2, OCT4 and NANOG in ovarian cancer tumor-initiating cells. Cancers (Basel) 2021;13:262.
10. Bollrath J, Greten FR. IKK/NF-kappaB and STAT3 pathways: central signalling hubs in inflammation-mediated tumour promotion and metastasis. EMBO Rep 2009;10:1314–9.
11. Karin M. NF-kappaB as a critical link between inflammation and cancer. Cold Spring Harb Perspect Biol 2009;1:a000141.
12. Annunziata CM, Stavnes HT, Kleinberg L, Berner A, Hernandez LF, Birrer MJ, et al. Nuclear factor kappaB transcription factors are coexpressed and convey a poor outcome in ovarian cancer. Cancer 2010;116:3276–84.
13. Annunziata CM, Davis RE, Demchenko Y, Bellamy W, Gabrea A, Zhan F, et al. Frequent engagement of the classical and alternative NF-kappaB pathways by diverse genetic abnormalities in multiple myeloma. Cancer Cell 2007;12:115–30.
14. Harrington BS, Annunziata CM. NF-κB signaling in ovarian cancer. Cancers (Basel) 2019;11:1182.
15. Hsu S, Kim M, Hernandez L, Grajales V, Noonan A, Anver M, et al. IKK-ε coordinates invasion and metastasis of ovarian cancer. Cancer Res 2012;72:5494–504.
16. Sun SC. Non-canonical NF-κB signaling pathway. Cell Res 2011;21:71–85.
17. Tegowski M, Baldwin A. Noncanonical NF-κB in cancer. Biomedicines 2018;6:66.
18. House CD, Jordan E, Hernandez L, Ozaki M, James JM, Kim M, et al. NFκB promotes ovarian tumorigenesis via classical pathways that support proliferative cancer cells and alternative pathways that support ALDH. Cancer Res 2017;77:6927–40.
19. Hufnagel DH, Wilson AJ, Saxon J, Blackwell TS, Watkins J, Khabele D, et al. Expression of p52, a non-canonical NF-kappaB transcription factor, is associated with poor ovarian cancer prognosis. Biomark Res 2020;8:45.
20. Uno M, Saitoh Y, Mochida K, Tsuruyama E, Kiyono T, Imoto I, et al. NF-κB inducing kinase, a central signaling component of the non-canonical pathway of NF-κB, contributes to ovarian cancer progression. PLoS One 2014;9:e88347.
21. House CD, Hernandez L, Annunziata CM. In vitro enrichment of ovarian cancer tumor-initiating cells. J Vis Exp 2015:52446.
22. Stirling DR, Swain-Bowden MJ, Lucas AM, Carpenter AE, Cimini BA, Goodman A. CellProfiler 4: improvements in speed, utility and usability. BMC Bioinf 2021;22:433.
23. Ljosa V, Sokolnicki KL, Carpenter AE. Annotated high-throughput microscopy image sets for validation. Nat Methods 2012;9:637.
24. Wang J, Sinnett-Smith J, Stevens JV, Young SH, Rozengurt E. Biphasic regulation of yes-associated protein (YAP) cellular localization, phosphorylation, and activity by G protein-coupled receptor agonists in intestinal epithelial cells: a novel role for protein kinase D (PKD). J Biol Chem 2016;291:17988–8005.
25. Hernandez L, Kim MK, Lyle LT, Bunch KP, House CD, Ning F, et al. Characterization of ovarian cancer cell lines as in vivo models for preclinical studies. Gynecol Oncol 2016;142:332–40.
26. Bairoch A. The cellosaurus, a cell-line knowledge resource. J Biomol Tech 2018;29:25–38.
27. Hagemann T, Wilson J, Kulbe H, Li NF, Leinster DA, Charles K, et al. Macrophages induce invasiveness of epithelial cancer cells via NF-kappa B and JNK. J Immunol 2005;175:1197–205.
28. Hong L, Wang S, Li W, Wu D, Chen W. Tumor-associated macrophages promote the metastasis of ovarian carcinoma cells by enhancing CXCL16/CXCR6 expression. Pathol Res Pract 2018;214:1345–51.
29. Chen R, Alvero AB, Silasi DA, Kelly MG, Fest S, Visintin I, et al. Regulation of IKKbeta by miR-199a affects NF-kappaB activity in ovarian cancer cells. Oncogene 2008;27:4712–23.
30. Dai L, Gu L, Ding C, Qiu L, Di W. TWEAK promotes ovarian cancer cell metastasis via NF-kappaB pathway activation and VEGF expression. Cancer Lett 2009;283:159–67.
31. Wu AY, Gu LY, Cang W, Cheng MX, Wang WJ, Di W, et al. Fn14 overcomes cisplatin resistance of high-grade serous ovarian cancer by promoting Mdm2-mediated p53-R248Q ubiquitination and degradation. J Exp Clin Cancer Res 2019;38:176.
32. Wang Y, Zong X, Mitra S, Mitra AK, Matei D, Nephew KP. IL-6 mediates platinum-induced enrichment of ovarian cancer stem cells. JCI Insight 2018;3:e122360.
33. Jordan KR, Sikora MJ, Slansky JE, Minic A, Richer JK, Moroney MR, et al. The capacity of the ovarian cancer tumor microenvironment to integrate inflammation signaling conveys a shorter disease-free interval. Clin Cancer Res 2020;26:6362–73.
34. Javellana M, Eckert MA, Heide J, Zawieracz K, Weigert M, Ashley S, et al. Neoadjuvant chemotherapy induces genomic and transcriptomic changes in ovarian cancer. Cancer Res 2022;82:169–76.
35. Winkles JA. The TWEAK-Fn14 cytokine-receptor axis: discovery, biology and therapeutic targeting. Nat Rev Drug Discov 2008;7:411–25.
36. Sliogeryte K, Thorpe SD, Lee DA, Botto L, Knight MM. Stem cell differentiation increases membrane-actin adhesion regulating cell blebability, migration and mechanics. Sci Rep 2014;4:7307.
37. Fan YL, Zhao HC, Li B, Zhao ZL, Feng XQ. Mechanical roles of F-actin in the differentiation of stem cells: a review. ACS Biomater Sci Eng 2019;5:3788–801.
38. Patra B, Lateef MA, Brodeur MN, Fleury H, Carmona E, Péant B, et al. Carboplatin sensitivity in epithelial ovarian cancer cell lines: the impact of model systems. PLoS One 2020;15:e0244549.
39. Bilbao M, Katz C, Kass SL, Smith D, Hunter K, Warshal D, et al. Epigenetic therapy augments classic chemotherapy in suppressing the growth of 3D high-grade serous ovarian cancer spheroids over an extended period of time. Biomolecules 2021;11:1711.
40. Wang Y, Zhao G, Condello S, Huang H, Cardenas H, Tanner EJ, et al. Frizzled-7 identifies platinum-tolerant ovarian cancer cells susceptible to ferroptosis. Cancer Res 2021;81:384–99.
41. Bensen RC, Gunay G, Finneran MC, Jhingan I, Acar H, Burgett AWG. Small molecule targeting of oxysterol-binding protein (OSBP)-related protein 4 and OSBP inhibits ovarian cancer cell proliferation in monolayer and spheroid cell models. ACS Pharmacol Transl Sci 2021;4:744–56.
42. Cheng E, Armstrong CL, Galisteo R, Winkles JA. TWEAK/Fn14 axis-targeted therapeutics: moving basic science discoveries to the clinic. Front Immunol 2013;4:473.
43. Pogge von Strandmann E, Reinartz S, Wager U, Müller R. Tumor-host cell interactions in ovarian cancer: pathways to therapy failure. Trends Cancer 2017;3:137–48.
44. Qian J, LeSavage BL, Hubka KM, Ma C, Natarajan S, Eggold JT, et al. Cancer-associated mesothelial cells promote ovarian cancer chemoresistance through paracrine osteopontin signaling. J Clin Invest 2021;131:e146186.
45. Hernandez L, Hsu SC, Davidson B, Birrer MJ, Kohn EC, Annunziata CM. Activation of NF-kappaB signaling by inhibitor of NF-kappaB kinase beta increases aggressiveness of ovarian cancer. Cancer Res 2010;70:4005–14.
46. Enwere EK, Lacasse EC, Adam NJ, Korneluk RG. Role of the TWEAK-Fn14-cIAP1-NF-κB signaling axis in the regulation of myogenesis and muscle homeostasis. Front Immunol 2014;5:34.
47. Dogra C, Changotra H, Mohan S, Kumar A. Tumor necrosis factor-like weak inducer of apoptosis inhibits skeletal myogenesis through sustained activation of nuclear factor-kappaB and degradation of MyoD protein. J Biol Chem 2006;281:10327–36.
48. Saitoh T, Nakayama M, Nakano H, Yagita H, Yamamoto N, Yamaoka S. TWEAK induces NF-kappaB2 p100 processing and long lasting NF-kappaB activation. J Biol Chem 2003;278:36005–12.
49. Sanz AB, Sanchez-Niño MD, Ortiz A. TWEAK, a multifunctional cytokine in kidney injury. Kidney Int 2011;80:708–18.
50. Winkles JA, Tran NL, Brown SA, Stains N, Cunliffe HE, Berens ME. Role of TWEAK and Fn14 in tumor biology. Front Biosci 2007;12:2761–71.

51. Chicheportiche Y, Bourdon PR, Xu H, Hsu YM, Scott H, Hession C, et al. TWEAK, a new secreted ligand in the tumor necrosis factor family that weakly induces apoptosis. J Biol Chem 1997;272:32401–10.
52. Burkly LC, Michaelson JS, Hahm K, Jakubowski A, Zheng TS. TWEAKing tissue remodeling by a multifunctional cytokine: role of TWEAK/Fn14 pathway in health and disease. Cytokine 2007;40:1–16.
53. Perez JG, Tran NL, Rosenblum MG, Schneider CS, Connolly NP, Kim AJ, et al. The TWEAK receptor Fn14 is a potential cell surface portal for targeted delivery of glioblastoma therapeutics. Oncogene 2016;35:2145–55.
54. Nakayama M, Kayagaki N, Yamaguchi N, Okumura K, Yagita H. Involvement of TWEAK in interferon gamma-stimulated monocyte cytotoxicity. J Exp Med 2000;192:1373–80.
55. Burkly LC, Michaelson JS, Zheng TS. TWEAK/Fn14 pathway: an immunological switch for shaping tissue responses. Immunol Rev 2011;244:99–114.
56. Méndez-Barbero N, Gutierrez-Muñoz C, Madrigal-Matute J, Mínguez P, Egido J, Michel JB, et al. A major role of TWEAK/Fn14 axis as a therapeutic target for post-angioplasty restenosis. EBioMedicine 2019;46:274–89.
57. Bird TG, Lu WY, Boulter L, Gordon-Keylock S, Ridgway RA, Williams MJ, et al. Bone marrow injection stimulates hepatic ductular reactions in the absence of injury via macrophage-mediated TWEAK signaling. Proc Natl Acad Sci U S A 2013;110:6542–7.
58. Maecker H, Varfolomeev E, Kischkel F, Lawrence D, LeBlanc H, Lee W, et al. TWEAK attenuates the transition from innate to adaptive immunity. Cell 2005;123:931–44.
59. Maymó-Masip E, Fernández-Veledo S, Garcia España A, Vázquez-Carballo A, Tinahones FJ, García-Fuentes E, et al. The rise of soluble TWEAK levels in severely obese subjects after bariatric surgery may affect adipocyte-cytokine production induced by TNFα. J Clin Endocrinol Metab 2013; 98:E1323–33.
60. Vendrell J, Chacón MR. TWEAK: a new player in obesity and diabetes. Front Immunol 2013;4:488.
61. Luo L, Zeng J, Liang B, Zhao Z, Sun L, Cao D, et al. Ovarian cancer cells with the CD117 phenotype are highly tumorigenic and are related to chemotherapy outcome. Exp Mol Pathol 2011;91:596–602.
62. Fukuda T, Fukuda R, Koinuma D, Moustakas A, Miyazono K, Heldin CH. BMP2-induction of FN14 promotes protumorigenic signaling in gynecologic cancer cells. Cell Signal 2021;87:110146.
63. Whitsett TG, Mathews IT, Cardone MH, Lena RJ, Pierceall WE, Bittner M, et al. Mcl-1 mediates TWEAK/Fn14-induced non-small cell lung cancer survival and therapeutic response. Mol Cancer Res 2014;12:550–9.
64. Itoigawa Y, Harada N, Harada S, Katsura Y, Makino F, Ito J, et al. TWEAK enhances TGF-β-induced epithelial-mesenchymal transition in human bronchial epithelial cells. Respir Res 2015;16:48.
65. Liu JY, Jiang L, He T, Liu JJ, Fan JY, Xu XH, et al. NETO2 promotes invasion and metastasis of gastric cancer cells via activation of PI3K/Akt/NF-κB/Snail axis and predicts outcome of the patients. Cell Death Dis 2019; 10:162.